AGU100 ADVANCING EARTH AND SPACE SCIENCE

Tectonics

RESEARCH ARTICLE
10.1029/2019TC005639

Key Points:
- Oligo-Miocene Central Cordillera diorite complex exhibit Sr-Nd isotope composition controlled by pelagic sediments
- Mio-Pleistocene igneous rocks exhibit Sr-Nd isotope composition controlled by the subducted Scarborough Seamount Chain basalts
- Temporal variations in isotope geochemistry for the Taiwan-Luzon magmatism mirror a tectonic transition and crustal maturation

Supporting Information:
- Supporting Information S1

Correspondence to:
H.-Q. Liu and Y.-G. Xu,
liuhaiquan@gig.ac.cn;
yigangxu@gig.ac.cn

Citation:
Liu, H.-Q., Yumul, G. P., Jr, Dimalanta, C. B., Queaño, K., Xia, X.-P., Peng, T.-P., et al. (2020). Western Northern Luzon isotopic evidence of transition from proto-south China Sea to South China Sea fossil ridge subduction. *Tectonics*, *39*, e2019TC005639. https://doi.org/10.1029/2019TC005639

Received 26 APR 2019
Accepted 20 NOV 2019
Accepted article online 26 NOV 2019

Western Northern Luzon Isotopic Evidence of Transition From Proto-South China Sea to South China Sea Fossil Ridge Subduction

Hai-Quan Liu[1,2,3], Graciano P. Yumul Jr[4], Carla B. Dimalanta[5], Karlo Queaño[6], Xiao-Ping Xia[1], Tou-Ping Peng[1], Jiang-Bo Lan[7], Yi-Gang Xu[1], Yi Yan[2], Juan Miguel R. Guotana[5], and Valerie Shayne Olfindo[5]

[1]State Key Laboratory of Isotope Geochemistry, Guangzhou Institute of Geochemistry, Chinese Academy of Sciences, Guangzhou, China, [2]Key Laboratory of Ocean and Marginal Sea Geology, Guangzhou Institute of Geochemistry, Chinese Academy of Sciences, Guangzhou, China, [3]Southern Marine Science and Engineering Guangdong Laboratory, Guangzhou, China, [4]School of Environmental Science and Management, University of the Philippines Los Baños, Laguna, Philippines, [5]Rushurgent Working Group, National Institute of Geological Sciences, College of Science, University of the Philippines Diliman, Quezon City, Philippines, [6]Department of Environmental Science, School of Science and Engineering, Ateneo de Manila University, Quezon City, Philippines, [7]State Key Laboratory of Ore Deposit Geochemistry, Institute of Geochemistry, Chinese Academy of Sciences, Guiyang, China

Abstract Temporal geochemical comparisons are conducted for representative magmatism from western Northern Luzon to reconstruct the Cenozoic tectonics. Oligo-Pleistocene magmas from western Northern Luzon display elemental and Sr-Nd-Hf-Pb-O isotope geochemistry similar to intraoceanic arc magmatism, consistent with derivation from the mantle wedge, coupled with fractional crystallization. Specifically, the Oligo-Miocene (~26.8–15.6 Ma) Central Cordillera diorite complex samples exhibit a negative correlation between Sr-Nd isotopes, consistent with mantle metasomatism by fluids/melts released from pelagic sediments. The Mio-Pleistocene samples (<~9 Ma) exhibit consistent $^{87}Sr/^{86}Sr$ ratios with variable ε_{Nd} and partially overlap with those of Scarborough seamount basalts, consistent with mantle metasomatism by fluids/melts released from the Scarborough seamount basalts, which are being subducted beneath Northern Luzon with the South China Sea fossil ridge. Temporal changes in Sr-Nd-Hf-Pb isotopes are also observed for the Taiwan-Luzon arc magmatism. The Oligo-Miocene (>~9 Ma) magmatism exhibit intraoceanic arc isotopic signatures, suggestive of a chemical imprint from subducted pelagic sediments. The Mio-Pleistocene (<~9 Ma) lavas display enriched mantle-type isotope compositions, consistent with an input of terrigenous sediment in the mantle. The temporal variations in Sr-Nd-Hf-Pb isotopes for the Taiwan-Luzon magmatism, combined with paleomagnetic evidence, mirror a transition from the Proto-South China Sea to the South China Sea fossil ridge subduction beneath western Northern Luzon at ~9 Ma. In addition, this study also highlights the importance of relatively enriched components in the lower plate in the maturation of overriding juvenile oceanic crust in an arc-continent collision system.

1. Introduction

Arc-continent collision has been widely accepted as an important mechanism for continental growth through earth history (Jahn, 2004; Sengör et al., 1993). The Luzon arc-Taiwan collisional system serves as a natural laboratory for studying the ongoing tectonic processes of arc-continent collision (Figure 1a, Teng, 1990; Huang et al., 1997; Shao et al., 2015). However, debate remains as to the tectonic history of western Northern Luzon with significant disagreement on the onset of the South China Sea subduction. One view suggests that the E-dipping subduction of South China Sea started in the late Oligocene based on regional geological and tectonic observations (Bachman et al., 1983; Hayes & Lewis, 1984; Wang, 2012). The other view suggests a subduction initiation in the early to middle Miocene evidenced by the enrichment trends of Sr-Nd isotope compositions (Polve et al., 2007), whereas the late Oligocene geologic records are related to the W-dipping subduction of West Philippine Sea plate along the Proto-East Luzon Trough (Wolfe, 1988; Bellon & Yumul, 2000; Yumul et al., 2003; Polve et al., 2007). Such a disagreement regarding the onset of South China Sea subduction largely stemmed from the paucity of evidence constraining the link between the subduction input and output in the Manila subduction system.

10.1029/2019TC005639

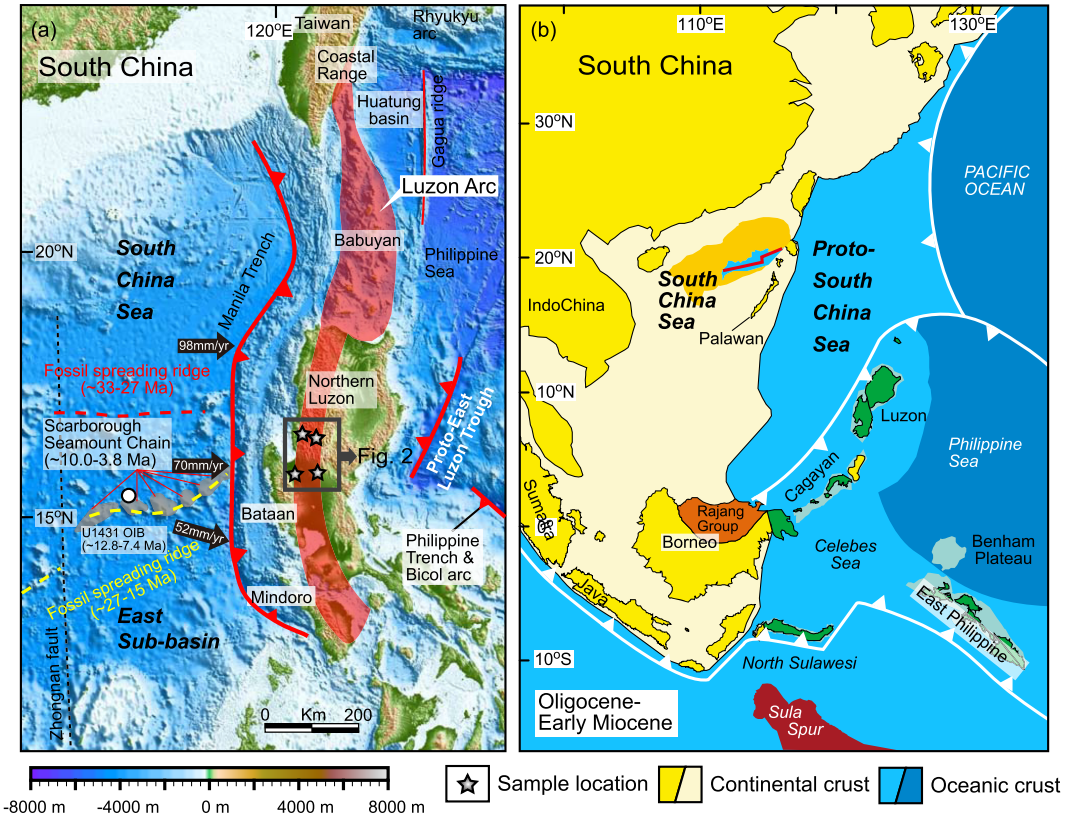

Figure 1. Tectonic framework showing main blocks and magmatism around the Luzon arc-Taiwan collision system (a) and paleogeographic reconstruction of southeastern Asia during Oligocene-early Miocene (b, modified from Hall, 2012). Yellow and red dashed lines (a) denote the locations of final fossil ridges (~27–15 Ma) and ridge jump (~33–27 Ma), respectively (Li et al., 2014).

Previous studies did not consider the contribution of the Proto-South China Sea to the magmatism and tectonics of western Northern Luzon by ascribing the pre-Miocene subduction to the modern South China Sea or the West Philippine Sea plate. The Mesozoic Proto-South China Sea was bounded by the Indochina-South China in the north and the Borneo-west Luzon in the south (Figure 1b, Taylor & Hayes, 1980; Hinz et al., 1991; Wu et al., 2016). It had been eliminated by subduction beneath northern Borneo-Cagayan-west Luzon during the Cenozoic (Hall & Breitfeld, 2017). The modern South China Sea is distinguished from other marginal oceanic basins in the west Pacific and normal oceanic plate by having a thick layer of terrigenous sediments, which had accumulated since its opening (Huang & Wang, 2006). In addition, it also features a seamount chain, known as the Scarborough Seamount Chain, that intruded the fossil spreading center of the South China Sea (Figure 1a, Taylor & Hayes, 1983; Tu et al., 1992; Zhang et al., 2017). The data obtained from the Bathymeter Sonar System (SeaBeam 2112), a deep-water multibeam sounding system, indicate that the Scarborough Seamount Chain is being subducted along with the fossil ridge beneath western Northern Luzon (Figure 1a; ~16°N, Pautot & Rangin, 1989; Li et al., 2004). Compared to mid-ocean ridge basalts (MORBs) in the region which exhibit depleted Sr-Nd isotopic signatures (Indian or depleted mantle-like, $^{87}Sr/^{86}Sr$ < ~0.7037, ε_{Nd} > ~+5; Hickey-Vargas et al., 2008; Zhang et al., 2018), the Scarborough seamount basalts and South China Sea sediments have relatively enriched Sr-Nd isotopic signatures (Scarborough basalts: $^{87}Sr/^{86}Sr$ = 0.703176 to 0.703922, ε_{Nd} = +3.0 to +5.5; sediments: $^{87}Sr/^{86}Sr$ = 0.71207 to 0.71499, ε_{Nd} = −13.0 to −9.3; McDermott et al., 1993; Li et al., 2003; Zhang et al., 2017). The enriched isotopic signatures are used to mark the South China Sea subduction, which in turn, can constrain the tectonic history of pre-South China Sea subduction.

In this paper, we first report geochemical data for representative of Oligocene-Pleistocene igneous rocks emplaced in western Northern Luzon and northern Bataan (Figure 2), which are interpreted to be derived from partial melts of the metasomatized mantle wedge. It is shown that the mantle source of the

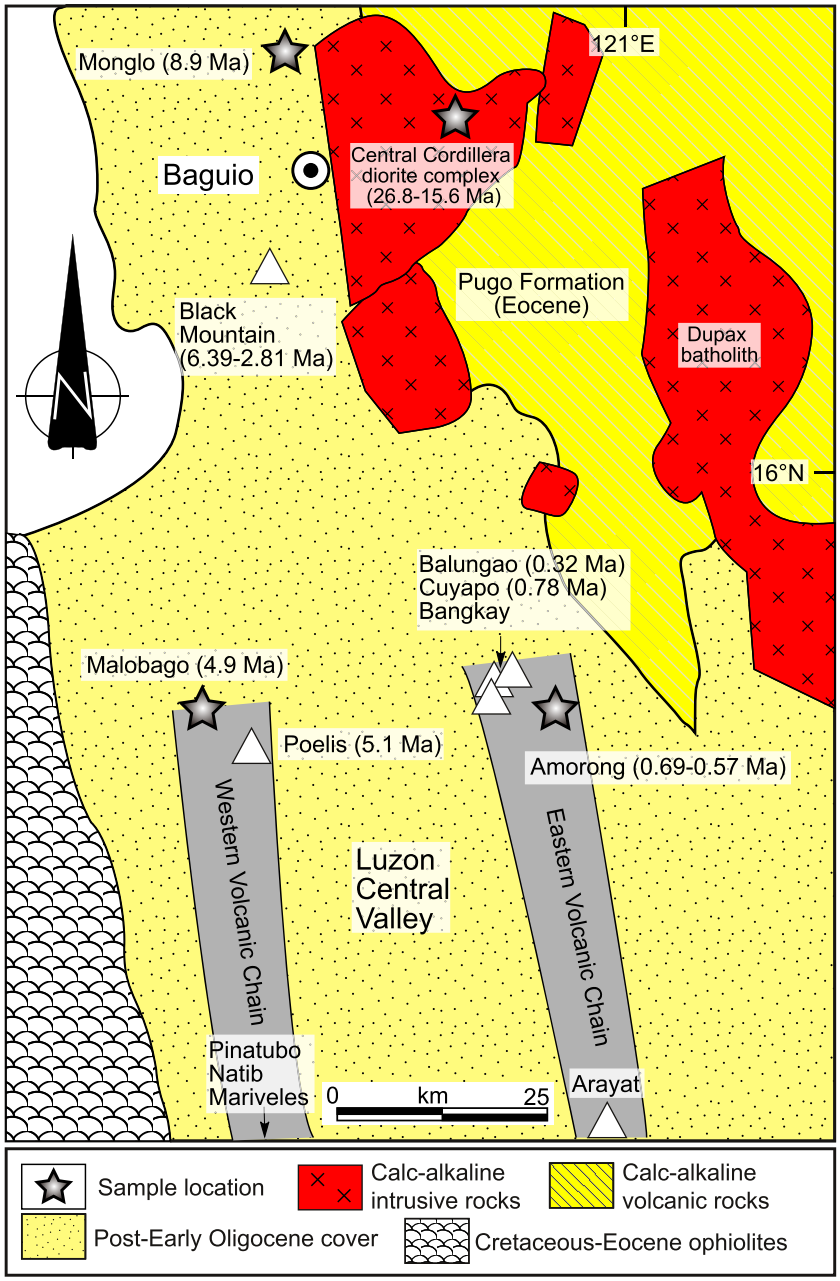

Figure 2. Sketch geologic map of western Northern Luzon (modified from Hollings, Wolfe, et al., 2011). Emplacement ages for the western northern Luzon magmas are from Encarnación et al. (1993), Bellon and Yumul (2000), Hollings, Cooke, et al. (2011), Waters et al. (2011), and this study.

Oligocene-early Miocene samples (~26.8–15.6 Ma) was metasomatized by fluids/melts derived from pelagic sediments, whereas the late Miocene-Pleistocene samples (<~9 Ma) involved contribution of fluids/melts derived from the subducted Scarborough seamount basalts. Combined with available data in the literature, dramatic changes in Sr-Nd-Hf-Pb isotope composition have been spotted for arc magmas emplaced in the Taiwan-Luzon area in the late Miocene (~9.0 Ma), which are contemporary with the presence of Scarborough seamount basalt signatures in the Miocene lavas. Finally, it is argued that the presence of seamount signatures and the changes in Sr-Nd-Hf-Pb isotope compositions for the Taiwan-Luzon magmatism marked a transition from the subduction of the Proto-South China Sea to the South China Sea fossil ridge beneath western Northern Luzon.

2. Geological Background

2.1. South China Sea and Proto-South China Sea

The South China Sea is a marginal basin that formed in the Oligocene to early Miocene (~33–15 Ma; Taylor & Hayes, 1983; Briais et al., 1993; Li et al., 2014). It is widely accepted that South China Sea seafloor spreading initially occurred in the East Sub-basin (~33–27 Ma) and was followed by a southward ridge jump and re-orientation of the spreading geometry from westward to southwestward ridge propagation (~27–15 Ma; Figure 1a, Briais et al., 1993; Huchon et al., 2001; Li et al., 2014; Ding & Li, 2016; Ding et al., 2018). The basaltic crust of the South China Sea has trace element features similar to the MORB and isotope compositions similar to Indian MORB (Zhang et al., 2018). After cessation of seafloor spreading, the Scarborough Seamount Chain (Figure 1a; 12.8–3.8 Ma, Wang et al., 2009; Xu et al., 2012; Zhang et al., 2017) was formed along the fossil ridge of South China Sea (Taylor & Hayes, 1980, 1983). The Scarborough seamount basalts exhibit oceanic island basalt-like geochemical composition (Tu et al., 1992; Zhang et al., 2017). Sedimentological studies on the South China Sea show that the highest sediment accumulation rate occurred in the Oligocene. Unlike open oceans and other small back-arc basins in the West Pacific, the South China Sea is characterized by thick terrigenous sediments on the continental shelf without large abyssal fans (Huang & Wang, 2006). The South China Sea is being subducted beneath the Huatung basin-Northern Luzon along the Manila Trench, with a convergence rate increasing linearly from ~52 mm/year at ~15^{o}N to ~98 mm/year at ~18^{o}N (Figure 1a, Tsai et al., 1981; Pautot & Rangin, 1989; Rangin et al., 1999). Bathymeter Sonar System survey reveals that the Scarborough Seamount Chain is currently being subducted with the South China Sea fossil spreading center at the intersection of Scarborough Seamount Chain and Manila Trench (Figure 1a; ~16^{o}N, Pautot & Rangin, 1989; Li et al., 2004).

The term Proto-South China Sea refers to a large Mesozoic oceanic embayment situated between Indochina-South China block in the north and Borneo in the south and predated the formation of the South China Sea (Figure 1b; Taylor & Hayes, 1980; Hinz et al., 1991). The existence of the Proto-South China Sea slab is still controversial due to the paucity of direct evidence (Hutchison, 2010). However, high-velocity anomalies beneath Borneo and Philippines near the mantle transition zone are interpreted as evidence of the existence of the subducted Proto-South China Sea (Hall & Breitfeld, 2017; Fan et al., 2017; Tang & Zheng, 2013). Sedimentary, structural, and magmatic records in northwestern Kalimantan and neighboring regions also argue for the existence of the Jurassic-Cretaceous Proto-South China Sea, which developed in the transition zone of the Tethys Ocean and the Paleo-Pacific Ocean (Wang et al., 2016). The Proto-South China Sea had been completely eliminated by subduction beneath the northern Borneo-Cagayan-west Luzon during the Eocene- Miocene (Hall & Breitfeld, 2017). Closure of the Proto-South China Sea along north Kalimantan is a diachronous, scissor-like southward subduction process that started from the west and propagated eastward during the late Cretaceous-Miocene (Wang et al., 2016).

2.2. Northern Luzon and Northern Bataan Segment of Luzon Arc

Northern Luzon is sandwiched between the Manila Trench to the west and the Proto-East Luzon Trough to the east (Figure 1a), both of which are associated with subduction of oceanic lithosphere. Northern Luzon experienced a northward drift from subequatorial latitudes to present-day latitude started from the late Oligocene-early Miocene, with a significant portion of the early Cenozoic occupied at low latitudes (Figure 1b, Queaño et al., 2007; Hall, 2012). The readers are referred to Hollings et al. (2011) and the included references for the details of Northern Luzon geologic background.

The Luzon arc comprises Miocene to recent arc volcanism stretching roughly N-S from the Coastal Range of Taiwan (24^{o}N) to Mindoro (13^{o}N) through west Luzon, Philippines, consisting of five distinct segments: Coastal Range, Babuyan, Northern Luzon, Bataan, and Mindoro (Figure 1a; Defant et al., 1989). The Luzon arc lavas exhibit striking latitudinal variations in Sr isotope composition, with lavas erupted in the Northern Luzon segment exhibiting low initial Sr isotopic ratios, whereas those erupted in Coastal Range, Babuyan, southern Bataan, and Mindoro segments have high initial Sr isotopic ratios (supporting information, Figure S1, Defant & Drummond, 1990)). The increase in Sr isotopic ratios for the Luzon arc lavas is attributed to an increasing input of continental crust materials in the mantle source (Castillo, 1996; Chen et al., 1990; Defant & Drummond, 1990; DuFrane et al., 2006; McDermott et al., 1993).

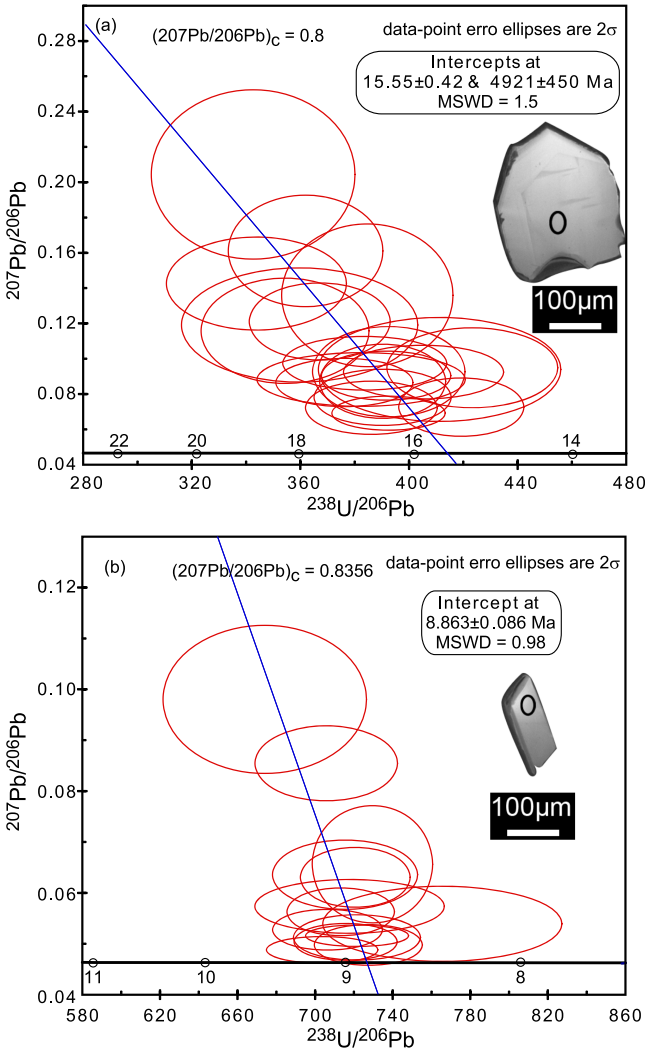

Figure 3. Tera-Wasserburg Concordia plots of SIMS U-Pb analyses for the Itogon quartz diorite (a, It15) and the Monglo dacite (b, Mla06). Insets are representative cathodoluminescence images showing their magmatic zonation and spots of in situ U-Pb (black cycles) isotopic analyses.

In the Baguio district, the Cretaceous ophiolitic basement is overlain by the Eocene Pugo Formation, a sequence of basaltic-andesitic volcanic rocks interbedded with sedimentary rocks (Hollings, Wolfe, et al., 2011; Peña, 1998; Schafer, 1954). The Pugo Formation is intruded by the Central Cordillera diorite complex (Figure 2; CCDC, or the Agno batholith in other literature, Balce et al., 1980) in the southernmost part of the Central Cordillera Ranges, occupying an area of ~300 km^2. The CCDC, representative of arc magmatism in western Northern Luzon during the Oligocene to Miocene, consists of six plutons, which are the Kadang trondhjemite, Itogon quartz diorite, Antamok diorite, Liang gabbro, Lucbuban gabbro, and Virac granodiorite (Cooke & Bloom, 1990; Hollings, Wolfe, et al., 2011; Shannon, 1979). Isotopic dating yielded Oligocene to early Miocene ages of 26.8 ± 0.4, 22.6 ± 0.5, and 20.2 ± 0.4 Ma for the CCDC (Encarnación et al., 1993; Waters et al., 2011; and references therein).

The volcanic centers of the Bataan segment form two parallel volcanic chains, the Western Volcanic Chain and the Eastern Volcanic Chain (Figure 2). The Western Volcanic Chain consists of Mount Malobago (4.9 ± 0.2 Ma), Poelis (5.1 ± 0.3 Ma) and Pitongbayog volcanoes in the north, and the Mount Pinatubo-Mount Natib-Mount Mariveles volcanoes together with parasitic volcanoes and andesitic to dacitic plugs and necks in the south (Figure 2) (Bellon & Yumul, 2000; Yumul et al., 2000, 2003). The Eastern Volcanic Chain is composed of the Mount Balungao (0.32 ± 0.03 Ma), Mount Cuyapo (0.78 ± 0.14 Ma), and Mount Amorong volcanoes (0.69–0.57 Ma) and the Mount Bangkay, a tuff cone deposit in the northern part, and Mount Arayat at the southern end (Figure 2; Bellon & Yumul, 2000; Yumul et al., 2000, 2003).

3. Results

Thirty-two igneous rocks were collected from western Northern Luzon for major, trace element and Sr-Nd-Hf-Pb isotopic study. Two samples from the Itogon (It15) and Monglo (Mla06) sections were prepared for zircon U-Pb and oxygen isotope analyses. Detailed petrographic information about the samples and analytical methods can be found in Text S1, Figure S2, and Table S1 (Encarnación et al., 1993; Whitehouse et al., 1997; Miyazaki & Shuto, 1998; Qi et al., 2000; Tanaka et al., 2000; Yumul et al., 2000; Bellon & Yumul, 2001; Ludwig, 2003; Weis et al., 2005; Wu et al., 2006; Payot et al., 2007; Polve et al., 2007; Sláma et al., 2008; Waters et al., 2011; Li et al., 2009, 2010, Li et al., 2010, 2013; GeoReM: http://georem.mpch-mainz.gwdg.de/; AIST: https://gbank.gsj.jp/geostandards/).

3.1. Zircon In Situ U-Pb Geochronology

Zircon U-Pb results and representative cathodoluminescence images are presented in Figures 3 and S3 and Table S2. Zircons from the Itogon quartz diorite (It15) and the Monglo dacite (Mla06) exhibit oscillatory zoning and have Th/U ratios of 0.27–3.72, consistent with crystallization from magmatic systems. Linear fits yield lower-intercept ages of 15.6 ± 0.4 (n = 20, MSWD = 1.5) and 8.9 ± 0.1 Ma (n = 16, MSWD = 0.98) for the Itogon and Monglo samples, respectively (Figure 3). These results suggest that the Itogon quartz diorites and the Monglo dacites in this study were emplaced at ~15.6 and ~8.9 Ma, respectively. Combined with previously published geochronologic results in the Itogon region (Text S2; Encarnación et al., 1993; Waters et al., 2011), our new data suggest that the CCDC have at least three phases of magmatism: ~26.8, ~22–20, and ~15.6 Ma. The zircon U-Pb dating result for the Monglo dacite is in agreement with a K-Ar age of 8.7 ± 0.2 within analytical error (Payot et al., 2007). Older, inherited $^{206}Pb/^{238}U$ zircon ages for the Monglo dacite range from 16.1 ± 0.4 to 46.6 ± 1.4 Ma (1σ; Table S2).

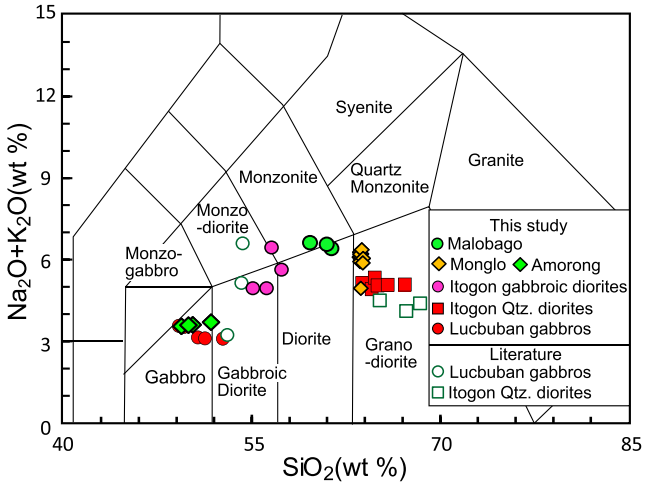

Figure 4. Alkalis versus silica contents for igneous rocks from western Northern Luzon. Major elements are corrected to 100 wt%. Classification is after Middlemost (1994). Data source: Lucbuban gabbros and Itogon quartz diorites are from Hollings, Wolfe, et al. (2011).

3.2. Whole-Rock Element Geochemistry

Whole-rock major and trace element data for the western Northern Luzon igneous rocks are reported in Table S3 and presented in Figures 4–7. Published data for the CCDC, Mindanao igneous rocks, experimental melts of metabasalt and amphibolite/eclogite melts, and hybrid melts are also presented in Figure 4–7 for comparison (see captions of Figure 4–7 for references). Samples from the Itogon region plot in the fields of gabbro, gabbroic diorite, and granodiorite (Figure 4). The granodiorites, however, are defined as quartz diorites based on their mineral assemblages (Table S1). According to the nomenclature of Middlemost (1994), the Lucbuban samples are gabbro to gabbroic diorite (Figure 4), but we name them gabbros based on their mineral assemblage (Figure S2c; Hollings, Wolfe, et al., 2011; and this study). The Itogon diorites (hereafter the Itogon diorites denote both the Itogon gabbroic diorites and the Itogon quartz diorites unless it is specified) are relatively evolved with low MgO (1.33–3.77 wt%) and high SiO_2 contents (54.65–66.91 wt%). In general, the three suites of CCDC samples exhibit a roughly positive correlation between CaO and MgO and negative correlations between Al_2O_3, CaO, MgO, Fe_2O_3, and TiO_2 versus SiO_2 contents (Figures 5b–5e, 5g–5h). The Lucbuban gabbros exhibit a negative correlation between Na_2O and SiO_2 (Figure 5f).

The Itogon gabbroic and quartz diorites have comparable Sr contents (415–493 ppm) contents (Table S3). However, the Itogon quartz diorites are distinct from the gabbroic diorites with low Y contents (<8.4 ppm) and therefore high Sr/Y ratios (>40, Table S3 and Figure 6a). The CCDC samples display a roughly positive correlation on a plot of Sr/Y versus silica (Figure 6d) and negative correlations on plots of Dy/Yb versus silica and Sr/Y versus Mg# (Figures 6e–6f). The Lucbuban gabbros and Itogon gabbroic diorites exhibit flat M-HREE (middle to heavy rare earth element) patterns. The Itogon quartz diorites exhibit slightly concave-upward patterns between MREEs and HREEs with $(Dy/Yb)_N < 1$ (Figure 7a and Table S3). In general, the CCDC intrusive rocks exhibit enrichment of large ion lithophile elements (LILEs, Rb, Ba, and Sr) relative to high field strength elements (HFSEs, Nb, Ta) on primitive mantle-normalized multielement diagrams (Figure 7b), similar to typical subduction-related magmas in Circum-Pacific arc zones.

On the total alkalis versus silica diagram, the Monglo, Malobago, and Amorong igneous rocks plot in fields of gabbro, monzonite, diorite, and granodiorite, equivalent to basalt, trachy-andesite, andesite, and dacite, respectively (Figure 4). For simplicity, the Malobago samples are defined as andesite and the Monglo samples are defined as dacite following Payot et al. (2007). The Monglo dacites exhibit high SiO_2 (>59.56 wt%), Al_2O_3 (>15.50 wt%), and Sr (>768 ppm) contents; Sr/Y (>143) and La/Yb ratios (>18); and low MgO (<3.46 wt%), Y (<6.9 ppm), and Yb contents (~0.4 ppm); and initial Sr isotope composition (<0.703623; Figure 6 and Table

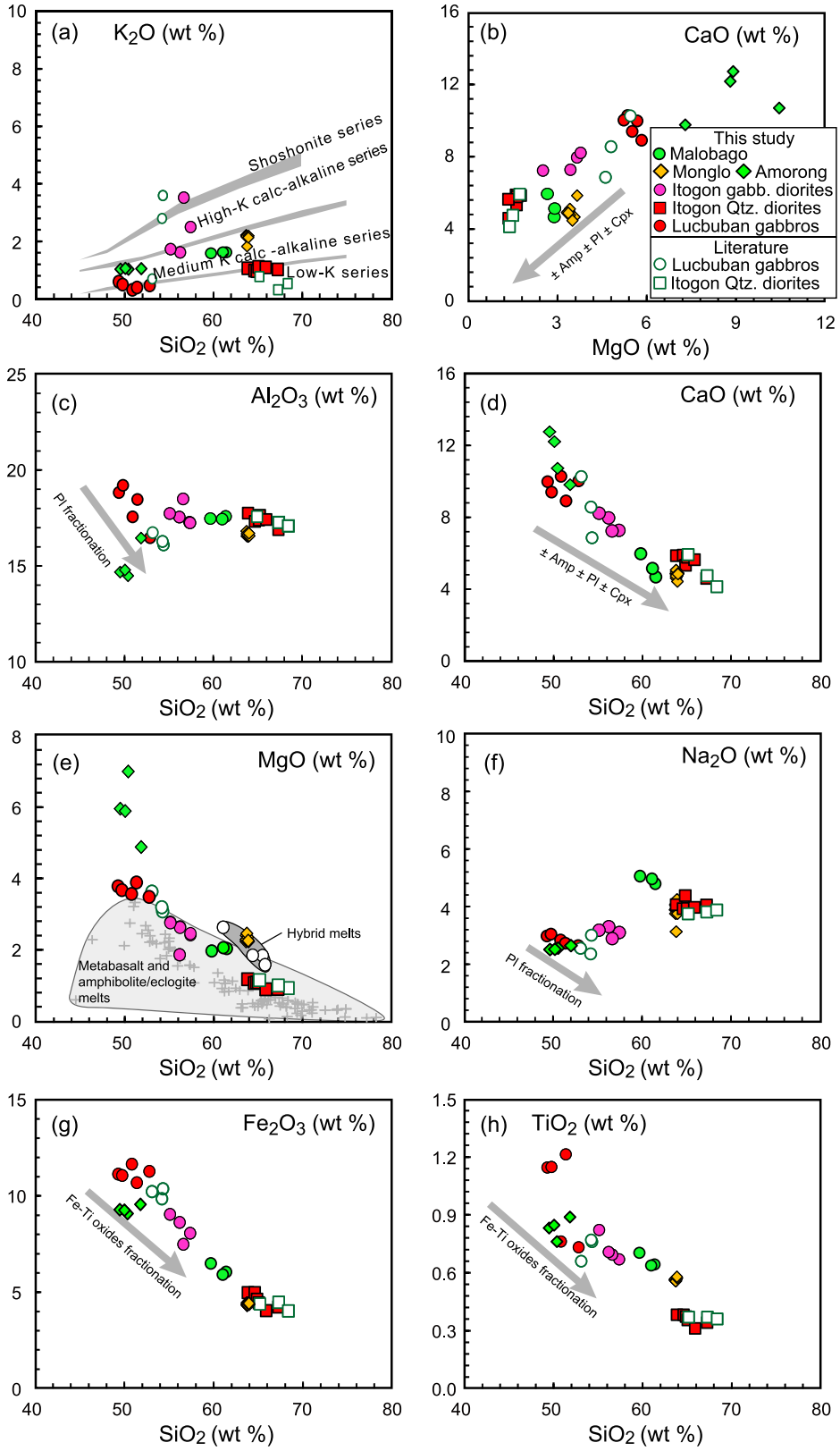

Figure 5. Variation of major elements versus SiO_2 for the western Northern Luzon igneous rocks. Data source: Lucbuban gabbros and Itogon quartz diorites, Hollings, Wolfe, et al. (2011); Experimental melts, Rapp and Watson (1995), Rapp et al. (1991), Winther and Newton (1991), Sen and Dunn (1994) and Rapp et al. (1999). Major elements are corrected to 100 wt%.

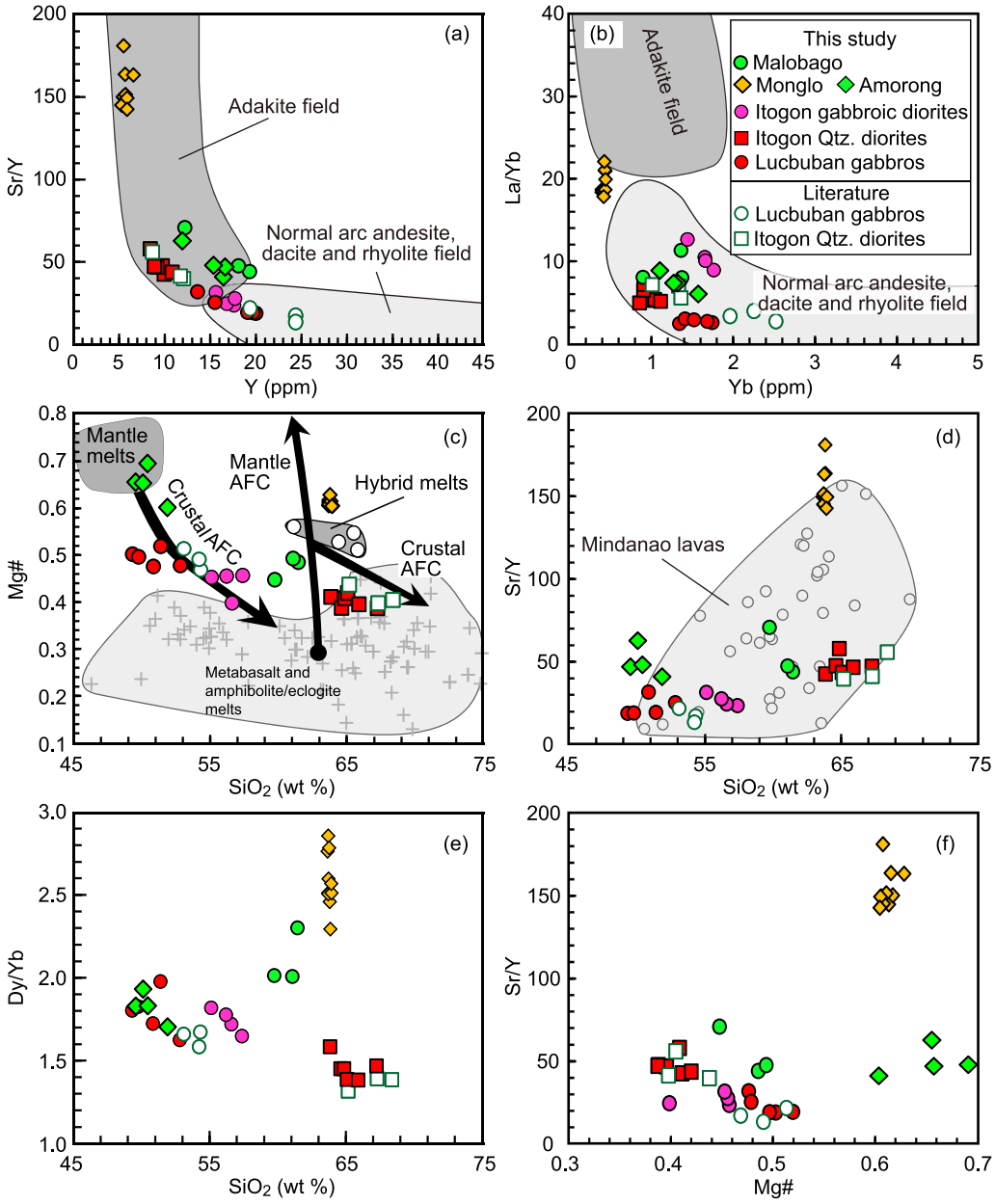

Figure 6. Sr/Y versus Y contents (a, modified from Defant & Drummond, 1990), La/Yb versus Yb contents (b, modified from Castillo, 2012), Mg# (c, modified from Stern & Kilian, 1996), Sr/Y (d) and Dy/Yb (e) versus SiO_2 contents, and Sr/Y versus Mg# diagrams (f) for the western Northern Luzon igneous rocks. Data source for the Lucbuban gabbros, Itogon quartz diorites, experimental melts are the same as in Figure 5. Chemical data for the Mindanao lavas are from Macpherson et al. (2006).

S3), resembling typical adakites (Defant & Drummond, 1990; Jégo et al., 2005; Polve et al., 2007). In Harker diagrams, the Amorong basalts essentially exhibit trends similar to those of the Lucbuban gabbros. However, the Amorong basalts have higher MgO and Mg# values than the Lucbuban gabbros (Figures 5, 6). The Malobago andesites and Monglo dacites are essentially similar to the Itogon diorites in major element contents with the exception of K_2O, MgO, and Na_2O contents (Figure 5). In particular, the Malobago andesites and the Monglo dacites have intermediate K_2O contents between the Itogon gabbroic diorites and quartz diorites (Figure 5a). The Monglo dacites exhibit high MgO contents and the highest Mg# values among the western Northern Luzon felsic rocks, plotting near the field of hybrid melts (Figures 5e and 6c), which represent the interaction products between slab-derived melts and mantle peridotites (Rapp et al.,

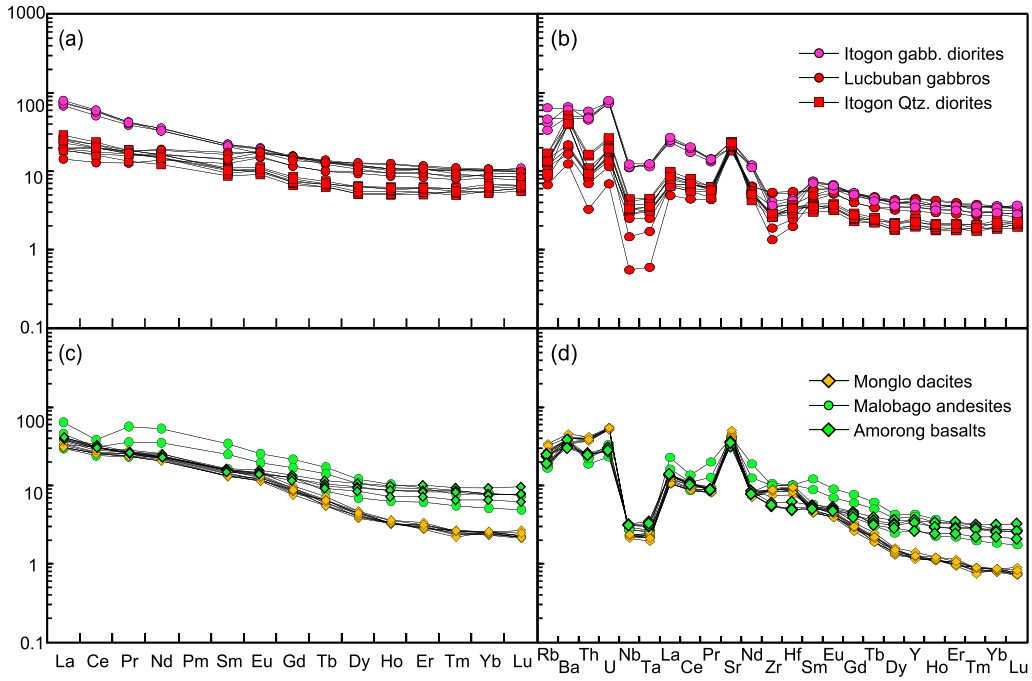

Figure 7. Whole rock Chondrite-normalized REE and primitive mantle-normalized multitrace element diagrams for the CCDC (a and b) and Monglo, Malobago, and Amorong igneous rocks (c and d). Normalization values are from Sun and McDonough (1989).

1999). The Malobago samples have the highest Na_2O contents of the western Northern Luzon igneous rocks (Figure 5f). The Monglo, Malobago, and Amorong igneous rocks essentially exhibit Chondrite-normalized REE and primitive mantle-normalized multielement patterns similar to those of the CCDC samples. However, the Monglo dacites have relatively steep REE patterns (Figures 7c–7d).

3.3. Whole-Rock Sr-Nd-Hf-Pb Isotope Geochemistry and Zircon In Situ Oxygen Isotope Geochemistry

Whole-rock Sr-Nd-Hf-Pb isotope compositions and zircon in situ oxygen isotope results are presented in Figures 8, 9 and Tables S3–S5. Isotopic data for igneous rocks and basement rocks (Zambales ophiolites and Huatung basalts) from the Taiwan-Luzon arc system and sediments from the South China Sea basin and the West Philippine Sea plate are also presented for comparison and discussion (Figure 8, see the caption for references). The western Northern Luzon igneous rocks have initial $^{87}Sr/^{86}Sr$ ratios from 0.703482 to 0.703875, $\varepsilon_{Nd}(t)$ values from 4.7 to 7.6, $\varepsilon_{Hf}(t)$ values from 12.3 to 17.8, Δ7/4 (=[($^{207}Pb/^{204}Pb$)-($^{206}Pb/^{204}Pb \times 0.1084 + 13.491$)] × 100; Hart, 1984) from 3.1 to 7.2 and Δ8/4 (=[($^{208}Pb/^{204}Pb$)-($^{206}Pb/^{204}Pb \times 1.209 + 15.627$)] × 100, Hart, 1984) from 32.1 to 54.1, respectively (Figure 8). In particular, the CCDC intrusive rocks exhibit a negative correlation on the Sr-Nd isotope diagram. Compared to the CCDC intrusive rocks, the Miocene-Pleistocene lavas exhibit essentially similar ranges of Nd-Hf-Pb isotope composition but marginally lower initial Sr isotope composition (Figures 8a–8b). However, the Miocene-Pleistocene lavas show consistent $^{87}Sr/^{86}Sr$ ratios over a variable range of ε_{Nd}, pointing to the field of South China Sea seamount basalts (Figures 8a–8b). Eocene-late Miocene igneous rocks and basement rocks from the Taiwan-Luzon arc system show intraoceanic arc signatures with narrow ranges in Sr-Nd-Pb isotopes (Figures 8c–8f). However, the late Miocene-Holocene Taiwan-Luzon magmas exhibit relatively large ranges in Sr-Nd-Hf-Pb isotope composition, plotting between the ranges of the South China Sea sediments and the Eocene-late Miocene magmas in northern Luzon (Figures 8c–8f). Terrigenous sediments from the South China Sea exhibit more radiogenic Sr-Pb but less radiogenic Nd isotopic ratios than pelagic sediments from the West Philippine Sea plate (Figures 8c–8f).

10.1029/2019TC005639

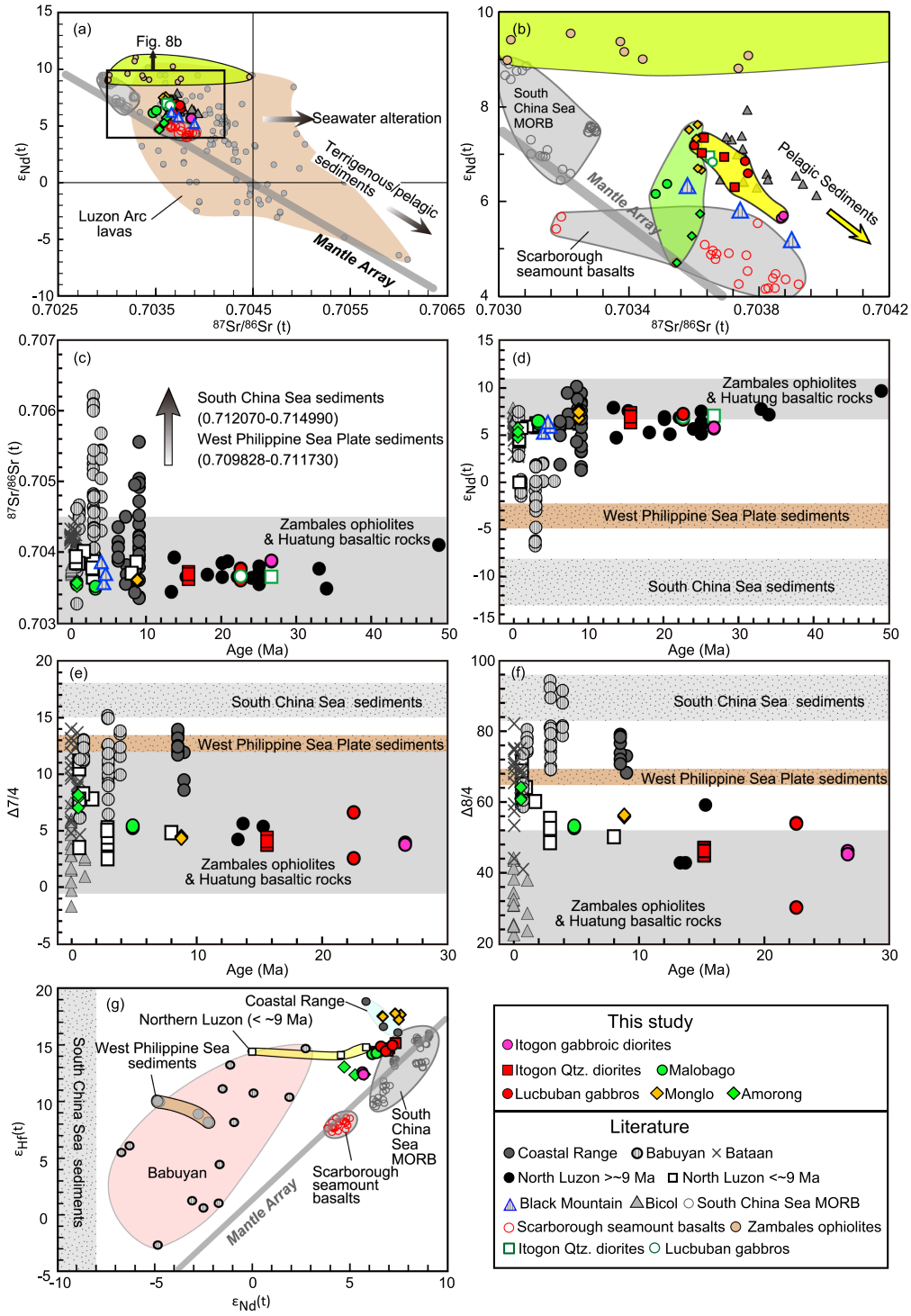

Figure 8. Plots of initial $\varepsilon_{Nd}(t)$ versus $^{87}Sr/^{86}Sr(t)$ (a and b), $^{87}Sr/^{86}Sr(t)$ (c), $\varepsilon_{Nd}(t)$ (d), Δ7/4 (e) and Δ8/4 (f) versus intrusion/eruption ages, and $\varepsilon_{Hf}(t)$ versus $\varepsilon_{Nd}(t)$ (g) for the Taiwan-Luzon arc system. Data source: Lucbuban gabbros and Itogon quartz diorites, Hollings, Wolfe, et al. (2011); Costal Range, Chen et al. (1990), Lai et al. (2017), Shao et al. (2015), Sun (1980); Babuyan, Chen et al. (1990), Marini et al. (2005), McDermott et al. (1993), Sun (1980), Vidal et al. (1989), Yang et al. (1996); Magmas older than 9 Ma from Northern Luzon, Hollings, Wolfe, et al. (2011), Knittel et al. (1988), Polve et al. (2007); Magmas younger than 9 Ma from Northern Luzon (including Black Mountain), DuFrane et al. (2006), Marini et al. (2005), McDermott et al. (1993), Mukasa et al. (1987), Polve et al. (2007), Hollings, Cooke, et al. (2011); Bataan, Bernard et al. (1996); DuFrane et al. (2006), Knittel et al. (1988), Knittel and Yang (1998), Mukasa et al. (1994); Bicol, DuFrane et al. (2006); South China Sea MORB, Zhang et al. (2018); Scarborough seamount basalts, Tu et al. (1992), Zhang et al. (2017); South China Sea sediments, McDermott et al. (1993), Li et al. (2003); West Philippine Sea plate sediments, Shimoda et al. (1998), Solidum et al. (2003), Vervoort et al. (2011); Zambales ophiolites, Encarnación et al. (1999); Huatung basaltic rocks, Hickey-Vargas et al. (2008).

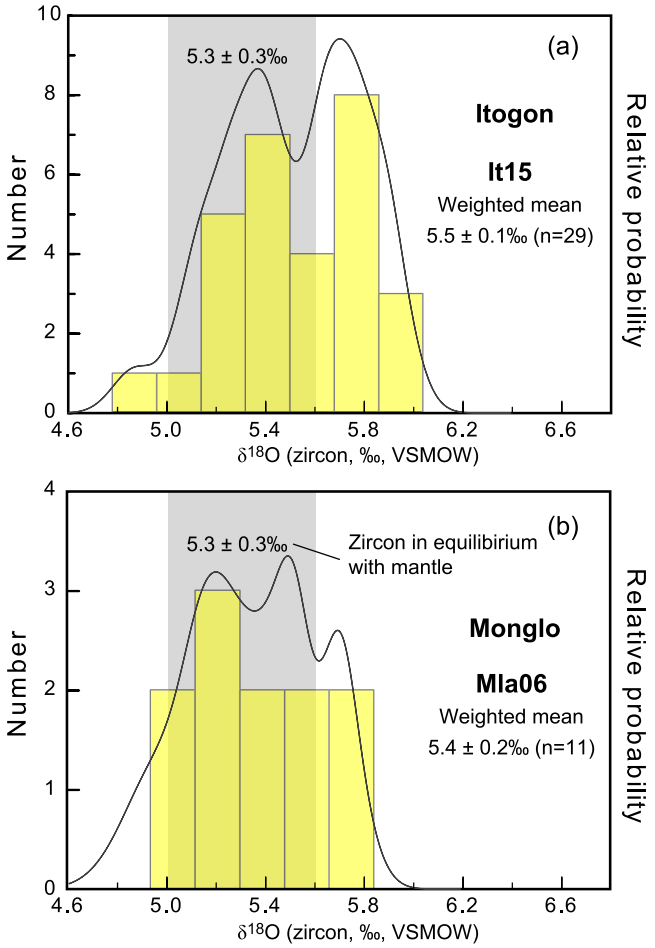

Figure 9. Plots of zircon in situ oxygen isotope composition for the Itogon diorite (a) and Monglo dacite (b). Value of zircon in equilibrium with mantle is from Valley et al. (2005).

Magmatic zircons from the Itogon quartz diorite and Monglo dacite have weighted mean $\delta^{18}O$ values of 5.5 ± 0.1‰ (n = 29) and 5.4 ± 0.2‰ (n = 11), respectively (Figure 9 and Table S5), identical to zircon in equilibrium with mantle within analytical errors (5.3 ± 0.3‰, Valley et al., 2005).

4. Discussion

4.1. Petrogenesis

4.1.1. Oligocene-Miocene CCDC Igneous Rocks

The Lucbuban gabbros exhibit a positive correlation between CaO versus MgO and negative correlations between Al_2O_3, CaO, MgO, and Na_2O versus SiO_2 (Figures 5b–5f), consistent with fractionation of clinopyroxene and plagioclase. Increase of K_2O and decreases of CaO, MgO, and Mg# with increasing SiO_2 for the Itogon diorites are indicative of fractionation of amphibole ± clinopyroxene (Figures 5a–5b, 5d–5e, and 6c). Negative correlations between TiO_2, Fe_2O_3, and SiO_2 for the CCDC intrusive rocks point to fractionation of Fe-Ti oxides (Figures 5g–5h).

Sr/Y ratios of the CCDC intrusive rocks correlate positively with SiO_2 contents, but negatively with Mg# (Figures 6d and 6f), suggesting differentiation of an amphibole- or garnet-bearing phase as in the case of the Mindanao lavas, Philippines (Castillo et al., 1999; Macpherson et al., 2006). A garnet-bearing assemblage is unable to reproduce the element signatures of the CCDC suite. Fractionation of a garnet-bearing assemblage would not only cause the depletion of Y from Sr but also induce depletion of HREEs from LREEs (high La/Yb ratios) and result in an increase of Dy/Yb with increasing SiO_2. This is because Y and HREEs are both strongly compatible with garnet. However, the CCDC intrusive rocks exhibit low La/Yb ratios (<13) and a decrease of Dy/Yb with the increase of SiO_2 (Figures 6b and 6e). In particular, the Itogon quartz diorites exhibit concave-upward patterns in the M-HREEs ($[Dy/Yb]_N < 1$; Figure 7a and Table S3). The decrease of Dy/Yb with differentiation and concave-upward patterns requires that a phase with $D_{Dy} < D_{Yb}$ (Rollinson, 1993), such as amphibole, was involved in the generation of the Itogon diorites.

The Itogon quartz diorites have Sr-Nd isotope composition similar to those of the Lucbuban gabbros. It is therefore argued that the Itogon quartz diorites are generated by differentiation of basaltic magma similar to the Lucbuban gabbros. The Itogon quartz diorite (It15) has zircon in situ $\delta^{18}O$ values identical to that of zircon in equilibrium with mantle (Figure 9a), which supports the interpretation that the Itogon quartz diorites are derived from mantle wedge-derived basaltic magmas. Likewise, the Itogon gabbroic diorites might be derived from differentiation of basaltic magma with more depleted Nd and elevated Sr isotope composition than the Lucbuban gabbros, as they exhibit more enriched Sr-Nd isotope composition than the Lucbuban gabbros (Figures 8a–8b).

4.1.2. Miocene-Pleistocene Igneous Rocks

Arc lavas with typical adakitic features in subduction zone could be generated by 1) remelting of thickened lower crust (Chung et al., 2003; Wang et al., 2007); 2) direct partial melting of subducting slab with or without mantle assimilation (mantle AFC) (Defant & Drummond, 1990; Kay, 1978; Rapp et al., 1999; Stern & Kilian, 1996); and 3) amphibole- or garnet-bearing assemblage differentiation of mantle wedge-derived basaltic magmatism with or without crustal assimilation (crustal AFC; Castillo et al., 1999; Macpherson et al., 2006).

The Monglo dacites could not be generated by partial melting of the Luzon crustal materials because they exhibit Nd isotopic ratios ($\varepsilon_{Nd}[t] < 7.6$) significantly lower than those of the Zambales ophiolites ($\varepsilon_{Nd}[t]$ = 8.8–11.0, Figures 8a–8b, Encarnación et al., 1999). Jégo et al. (2005) proposed that the Monglo dacites were derived from partial melting of eclogite converted from subducted oceanic metabasalts given their

significant depletion in Y and HREEs. Polve et al. (2007) supported this model and argued that the Monglo dacites were generated by partial melting of the subducted South China Sea basaltic crust. However, recent research on seafloor basalts recovered from the International Ocean Discovery Program Expedition 349 shows that the South China Sea MORB have Sr-Nd isotope composition (Zhang et al., 2018) different from those of the Monglo dacites (Figures 8a–8b). In addition, oceanic lithosphere is very heterogeneous in oxygen isotope composition ($\delta^{18}O = -15 - +42$ ‰) because of extensive near-surface hydrothermal alteration and weathering (Bindeman et al., 2005; Valley et al., 2005). Similar diversity would be expected for melts derived from subducted slabs. However, magmatic zircon grains from the Monglo adakite display a narrow range of zircon $\delta^{18}O$ values (5.0–5.7 ‰) with a weighted mean identical to zircon in equilibrium with mantle (Figure 9b; Valley et al., 2005), suggestive of mantle partial melts (Bindeman et al., 2005). Another explanation for the narrow mantle-like zircon $\delta^{18}O$ values for the Monglo dacite is the slab-derived melts have reached complete re-equilibration with the mantle wedge (Bindeman et al., 2005). This seems reasonable as the Monglo dacites display Mg# values and SiO_2 contents near those of experimental hybrid melts (Figures 5e and 6c), which represents an interaction between slab-derived melts and mantle peridotites (Rapp et al., 1999; Stern & Kilian, 1996). However, some adakitic lavas from modern arcs exhibit significant excesses of ($^{226}Ra/^{230}Th$), ($^{234}U/^{230}Th$), and ^{10}Be (Sigmarsson et al., 1998, 2002), suggesting that the melting and transfer rates to the surface may be rapid (10^3–10^4 year) and would not allow the magmas to reach a complete equilibrium between the ascending flow and mantle wedge (Bindeman et al., 2005). Thus, the Monglo dacites could not be generated by direct partial melting of a subducting slab.

Fractionation of an amphibole-bearing assemblage of mantle-derived basaltic magma will not yield the REE patterns of the Monglo dacites. Specifically, separation of these phases from the magmatic system would produce a negative correlation between Dy/Yb versus SiO_2 and flat to concave-upward patterns in M-HREEs ($[Dy/Yb]_N < 1$), like those of the CCDC intrusive rocks. However, no such correlation and pattern are observed for the Monglo dacites. In particular, the Monglo dacites exhibit steep REE patterns ($[Dy/Yb]_N > 1$, Figure 7c and Table S3), which need differentiation of a garnet-bearing assemblage rather than an amphibole-bearing assemblage (Macpherson et al., 2006). We therefore argue that the Monglo dacites are derived from mantle-derived basaltic magmas coupled with garnet-bearing assemblage differentiation. Fractionation of a garnet-bearing assemblage is plausible for the Monglo dacites as geophysical and geochemical data show that crustal thickness in western Northern Luzon is ~30 km (Dimalanta & Yumul, 2008), which critically meets the requirement of garnet-bearing assemblage fractionation.

The Malobago andesites exhibit nearly consistent K_2O, Al_2O_3, and MgO contents with increasing silica (Figures 5a,5c, and 5e), suggesting limited fractionation of amphibole. Decreases of CaO and Na_2O with increasing silica (Figures 5d and 5f) are consistent with plagioclase fractionation. This is supported by the negative correlation between Sr/Y and silicate (Figure 6d), as fractionation of plagioclase-bearing assemblages would lead to a decrease of Sr/Y and an increase of SiO_2 (Defant & Drummond, 1990). Negative correlations between Fe_2O_3, TiO_2, and SiO_2 indicate fractionation of Fe-Ti oxides for the Malobago samples (Figures 5g–5h). These geochemical characteristics, similar to those of normal arc lavas defined by Defant and Drummond (1990), collectively suggest that the Malobago andesites are derived from low-pressure differentiation of basaltic magmas.

The Amorong basalts exhibit the highest CaO, MgO contents and Mg# values among the western Northern Luzon arc magmas (Figures 5d–5e and 6c), suggesting limited crystal fractionation. In particular, the Amorong basalts plot at the right end of fractionation trend of amphibole ± plagioclase ± clinopyroxene on a plot of CaO versus MgO (Figure 5b) and partially overlap with mantle melts in the plot of Mg# versus SiO_2 (Figure 6c, Stern & Kilian, 1996). These features, combined with the lack of amphibole in thin sections (Figure S2f), suggest that the Amorong basalts are relatively primitive and have undergone limited fractional crystallization of olivine, clinopyroxene, and plagioclase. Flat HREE patterns suggest that the Amorong basalts are derived from partial melting of spinel-facies mantle peridotites (Mckenzie & O'Nions, 1991).

4.2. Isotopic Variations: Crustal Contamination or Source Contamination?

In general, post-magmatic alteration of the Sr-Nd-Pb isotope composition of the western Northern Luzon igneous rocks is negligible because the western Northern Luzon samples are essentially fresh in thin section and there is no correlation between Sr-Nd-Pb isotope composition and loss on ignition (Figures S2 and S4,

Text S3). Figures 8a–8b illustrate a negative correlation for the Oligocene-Miocene CCDC samples and a nearly vertical array for the Miocene-Pleistocene samples, respectively. In western northern Luzon, two mechanisms could be responsible for the Sr-Nd isotopic variations: 1) crustal contamination (Hollings, Wolfe, et al., 2011) and 2) source contamination by the subducted slab, including basaltic crust (MORB, Polve et al., 2007), terrigenous/pelagic sediments (Defant & Drummond, 1990; Knittel et al., 1988), and seamounts (Hollings et al., 2011; Hollings et al., 2013).

Lower crustal contamination or assimilation could not reproduce the Sr-Nd isotopic variations of the western Northern Luzon igneous rocks. This is because the Luzon basement rocks, represented by the Zambales ophiolitic mafic-ultramafic rocks, exhibit Sr-Nd contents significantly lower than and Sr-Nd isotope composition different from those of the western Northern Luzon igneous rocks (Figures 8a–8b and Table S3; Zambales: Sr < 88.4 ppm, Nd < 3.1 ppm; western Northern Luzon: Sr = 373–1,070 ppm, Nd = 5.4–41.2 ppm; Encarnación et al., 1999). A positive correlation between $^{87}Sr/^{86}Sr$ and silica and a negative correlation between $\varepsilon_{Nd}(t)$ and silica would be expected if the western Northern Luzon samples suffered upper crustal contamination, as upper crust generally has high $^{87}Sr/^{86}Sr$ ratios and SiO_2 contents and low ε_{Nd} values (Taylor et al., 1983). However, there is no such correlation observed among each suite of the western Northern Luzon igneous rocks (Figure S5), suggesting that upper crustal contamination is minor.

Source contamination by subducted oceanic crust is also not a viable option to reproduce the Sr-Nd isotopic variations. On one hand, fresh basaltic crust from a normal oceanic slab is thought to have geochemical composition similar to unaltered mantle wedge (MORB, Kelley et al., 2006), which would have little impact on the geochemical composition of subduction-related magmatism. On the other hand, Sr isotopic ratios of basaltic crust is preferentially increased by seawater-rock interaction during seafloor spreading (Delacour et al., 2008). If the mantle source of western Northern Luzon igneous rocks had been subjected to metasomatism by altered oceanic crust-derived fluids/melts, a horizontal trend with increasing Sr isotopic ratios but relatively consistent $\varepsilon_{Nd}(t)$ values comparable with those of MORB would be expected in the Sr-Nd isotopes diagram. However, there is no such trend observed for the western Northern Luzon samples.

Contamination of seafloor sediment (pelagic and/or terrigenous sediment) in mantle source would produce a negative correlation between Sr-Nd isotopes because subducted sediment generally has higher Sr and lower Nd isotopic ratios than the mantle (Plank & Langmuir, 1998). This is illustrated by the negative correlations of the Luzon arc and Bicol arc lavas in Figures 8a–8b, which have been interpreted as a modification of the mantle source by subducted sediments (Castillo, 1996; Chen et al., 1990; Defant & Drummond, 1990; Dufrane et al., 2006). Although the Bicol and Luzon arc lavas display negative Sr-Nd isotope correlations, the Bicol lavas are distinguished from the Luzon arc lavas by unradiogenic Sr but radiogenic Nd isotope compositions (Figures 8c–8d). This is because the mantle source of the Bicol arc lavas was subjected to a chemical imprint from subducted pelagic sediments, which contain little or no continental crustal component (Defant & Drummond, 1990; Knittel et al., 1988), whereas the mantle source of the Luzon arc lavas underwent input of South China Sea sediments, which contain a significant portion of enriched continental components (Defant & Drummond, 1990; Knittel et al., 1988; McDermott et al., 1993). The CCDC intrusive rocks and other Eocene-late Miocene magmas (~49–9 Ma) have unradiogenic Sr-Pb isotope compositions but radiogenic Nd isotope composition, similar to those of the Bicol arc lavas (Figure 8). This is consistent with a chemical imprint from subducted pelagic sediments and lack of a continental crustal input (Defant & Drummond, 1990; Knittel et al., 1988). Such an interpretation is supported by the newly acquired Pb-Hf isotope composition for the CCDC intrusive rocks. The CCDC intrusive rocks display unradiogenic Pb isotope composition (low $\Delta 7/4$ and $\Delta 8/4$ values) comparable to Bicol arc lavas (Figures 8e–8f) and radiogenic Hf isotope composition (Figure 8g), consistent with control of fluids/melts released from pelagic sediments.

Fluids/melts derived from the subducted South China Sea terrigenous/pelagic sediments will not generate the Sr-Nd isotopic characteristics of the late Miocene-Pleistocene western Northern Luzon samples, which delineate a nearly vertical trend with the Amorong basalts overlapping with the Scarborough seamount basalts. This suggests contribution of Scarborough seamount basalts to the source, which is consistent with the geophysical observation that the Scarborough Seamount Chain is currently being subducted beneath western Northern Luzon-northern Bataan (~16°N, Figure 1a; Pautot & Rangin, 1989; Fan et al., 2014; Li et al., 2004). This interpretation is supported by independent geochemical studies of the Black Mountain Complex, Baguio District. Three relatively primitive basaltic samples from the Black Mountain Complex

display Sr-Nd isotopes close to those of the Scarborough seamount basalts (Figures 8a–8b), suggesting mantle metasomatism by subducted seamount basalt-derived melts (Hollings et al., 2013, Hollings, Cooke, et al., 2011). Therefore, the nearly vertical trend exhibited by the late Miocene-Pleistocene lavas can be best explained as a consequence of metasomatism by fluids/melts derived from the subducted Scarborough seamount basalts.

4.3. Tectonic Transition From Proto-South China Sea to South China Sea Fossil Ridge Subduction

Multidisciplinary study of paleomagnetism, structure, geochronology, and geochemistry on North Luzon (Hollings, Wolfe, et al., 2011; Queaño et al., 2007) demonstrated that the Oligocene-Miocene western Northern Luzon magmatism (>~9 Ma) was probably related to E-dipping subduction of the South China Sea (Balce et al., 1980; Hayes & Lewis, 1984; Polve et al., 2007). However, this hypothesis might be inappropriate as terrigenous sediments had been deposited on the periphery of the South China Sea basin since the Oligocene (Huang & Wang, 2006), which are characterized by extremely elevated Sr-Pb and depleted Nd isotope composition (Figures 8c–8f; McDermott et al., 1993; Li et al., 2003). Involvement of these terrigenous sediments would dramatically modify the Sr-Nd-Hf-Pb isotope composition of the mantle wedge as in the case of the late Miocene to Recent Luzon arc lavas (Figure 8; Defant & Drummond, 1990; McDermott et al., 1993; Castillo, 1996; DuFrane et al., 2006). However, no contribution from the South China Sea terrigenous sediments is identified in the CCDC intrusive rocks and other Oligocene-late Miocene western Northern Luzon magmas (Figure 8), inconsistent with metasomatism by fluids/melts released from the South China Sea terrigenous sediments. In addition, paleomagnetic data for the Eocene-Miocene Luzon sedimentary and igneous rocks show that Northern Luzon mainly occupied low, subequatorial latitudes during the Eocene to middle Miocene (<~10^{o}N, Queaño et al., 2007). However, the Eastern Sub-basin was still located at a latitude of >~12^{o}N (Figures 1b and 10a; Queaño et al., 2007; Yuan et al., 1994). This paradox could be reconciled if there was another oceanic crust/basin located between the present South China Sea and Luzon Island before the E-dipping South China Sea subduction was initiated. The predicted Mesozoic Proto-South China Sea, located between the Indochina-South China and the Borneo-Cagayan-Luzon (Figures 1b and 10a, Hall & Breitfeld, 2017), meets the requirement of the E-dipping subduction. Although direct evidence is still missing, multidisciplinary evidence from sedimentary, structural, magmatic, and geophysical research supports the existence of the Proto-South China Sea, which had been eliminated by southeastward subduction along the Borneo-Cagayan-Luzon trench during the Cenozoic (Wang et al., 2016; Tang & Zheng, 2013; Hall & Breitfeld, 2017; Fan et al., 2017). We propose that subduction of the Proto-South China Sea was responsible for the generation of the CCDC intrusive rocks (Figures 10a and 11a). Other Oligocene-late Miocene western Northern Luzon magmas (~34–9 Ma) show Sr-Nd-Pb isotope composition comparable with those of the CCDC samples, suggesting that they might share similar petrogenesis with those of the CCDC and be controlled by the Proto-South China Sea subduction.

The occurrence of Scarborough Seamount Chain signatures in the Liw-Liw Creek dikes of the Black Mountain Complex leads Hollings, Cooke, et al., 2011, Hollings et al., 2013) to suggest that the South China Sea fossil ridge subduction beneath western Northern Luzon started at ~4.5 Ma. However, the Sr-Nd isotopic features for the Monglo, Malobago, and Amorong igneous rocks suggest that the Scarborough seamount signatures appeared at an earlier time than those of Black Mountain complex. Combined with Bathymeter Sonar System survey observation that the Scarborough Seamount Chain is being subducted with the South China Sea fossil ridge beneath western Northern Luzon (Li et al., 2004; Pautot & Rangin, 1989), the presence of Scarborough Seamount Chain geochemical signatures at ~9 Ma in the Monglo dacites marked the initial subduction of the South China Sea fossil ridge beneath western Northern Luzon. This is nearly contemporary with the dramatic increases of Sr-Pb isotopic ratios and decrease of $\varepsilon_{Nd}(t)$ for the Luzon arc magmatism, consistent with metasomatism of the South China Sea terrigenous sediment-derived fluids/melts in the mantle (Castillo, 1996; Chen et al., 1990; Knittel & Defant, 1988; Marini et al., 2005; McDermott et al., 1993). We therefore propose a transition from the Proto-South China Sea subduction to the South China Sea subduction beneath the Northern Luzon-Huatung basin at ~9 Ma (Figures 10b and 11b–11c).

The onset of the South China Sea fossil ridge subduction initiation must have started at an earlier time than the first appearance time of Scarborough Seamount Chain signatures in the Luzon arc lavas, as it takes time for subducted components at trench to recycle back to the surface through arc magmatism. Combined with subduction rate and angle and trench-arc distance, the onset time of the South China Sea fossil ridge

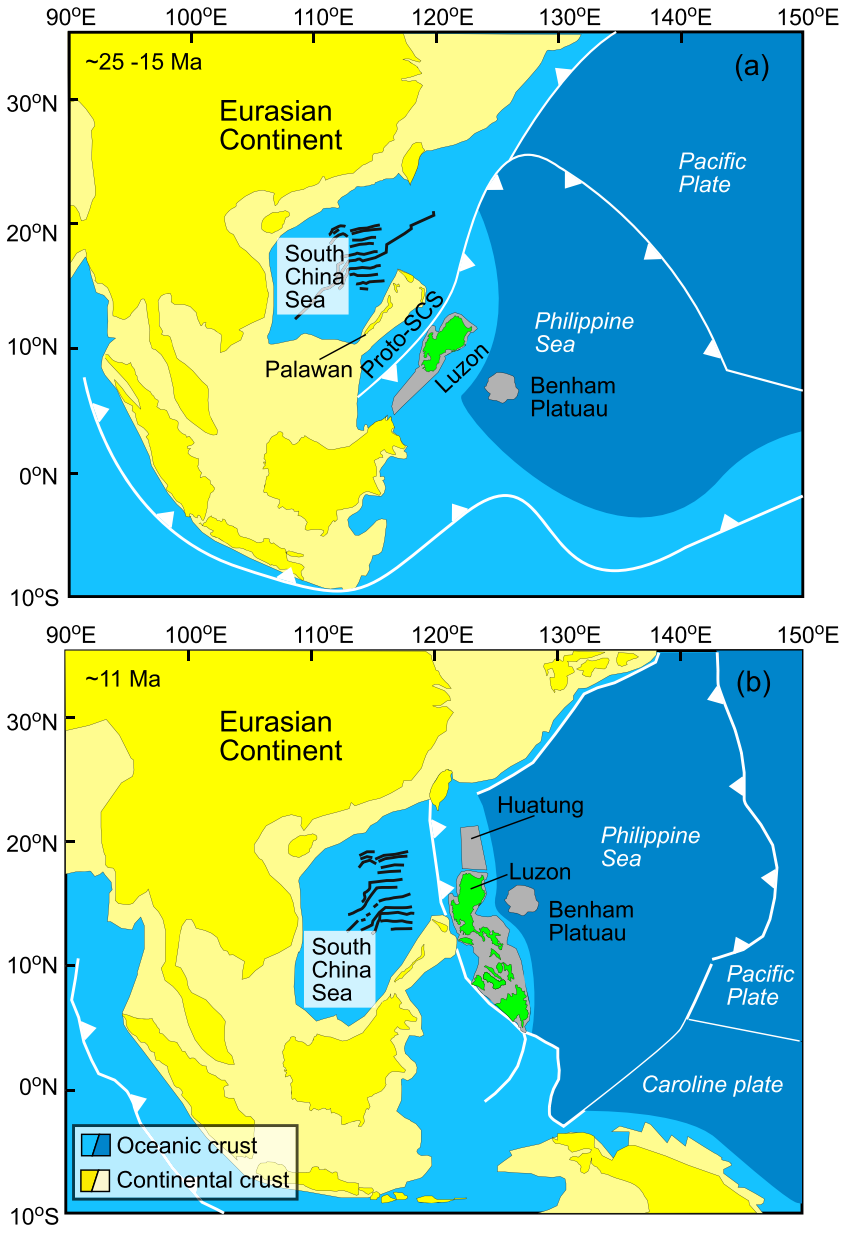

Figure 10. Schematic geologic map (modified from Queaño et al., 2007 and Hall, 2012) showing a tectonic transition from the Proto-South China Sea subduction (a) to the South China Sea subduction (b) beneath western Northern Luzon at ~11 Ma. The Proto-SCS denotes Proto-South China Sea.

subduction initiation can be estimated. The subduction rate and angle at ~16°N are assumed to be ~70 mm/year and ~24° respectively (Figures 1a and 11b–11c, Rangin et al., 1999; Li et al., 2004; Gao et al., 2012; Fan et al., 2014). The distance between the intersection and the Monglo dacites is ~150 km (Figures 1a and 11b) allowing a slab length ~164 km to be estimated (Figure 11b). Assuming that the South China Sea subduction rate and angle are constant, it would take at least ~2.3 Myrs until the subducted seamount basalts recycled back to the Luzon arc at ~16°N. Then the onset time of South China Sea fossil ridge subduction initiation is presumed to be ~11.3 Ma at ~16°N.

4.4. Implications for Crustal Growth

The Luzon arc basement rocks, represented by the Zambales Ophiolites to the south and Huatung basaltic rocks to the north, have juvenile arc crust affinity with low Sr-Pb and high Nd isotopic ratios (Figures 8c–8f).

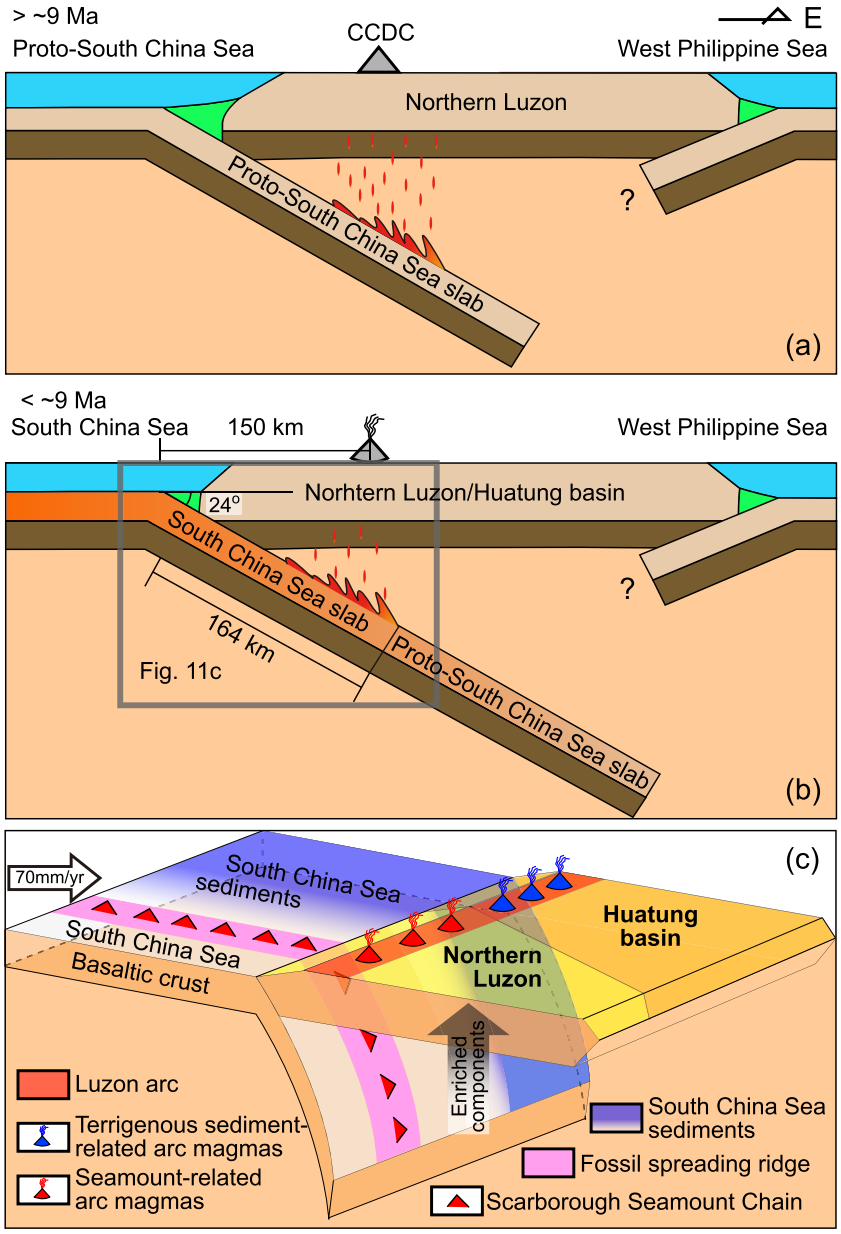

Figure 11. Cartoons showing the tectonic transition from the Proto-South China Sea subduction (a) to the South China Sea fossil ridge subduction (b, c). (c) A three-D cartoon illustrating the maturation process of the juvenile Luzon arc by incorporation of relatively enriched components such as terrigenous sediments and seamount basalts from the subducted South China Sea.

Similarly, the Eocene-late Miocene magmas also display relatively juvenile signatures with Sr-Nd-Pb isotope compositions resembling those of the Luzon arc basement rocks (Figures 8c–8f). However, the Miocene to recent (<~9 Ma) Luzon arc lavas exhibit Sr-Nd-Pb isotopic signatures pointing to the contribution of the South China Sea seamount basalts and terrigenous sediments (Figures 8a–8f). This indicates that relatively enriched components in the subducted South China Sea have contributed to the maturation of the juvenile Luzon arc crust. Maturation of juvenile oceanic crust by incorporation of enriched components in the lower plate has also been proposed in the Banda arc-continent collision system (Elburg et al., 2004; Vroon et al., 1993). Geochemical studies indicate that the subducted Australian continental materials, either as sediment or continental crust were responsible for the enriched Sr-Nd-Pb isotopic signatures for the Banda arc lavas (Elburg et al., 2004; Vroon et al., 1993). Whereas studies of numerous subduction systems emphasize the

significance of ancient crustal materials in the upper plate in relation to the maturation of juvenile oceanic crust (Ducea et al., 2015; Tang et al., 2019), the Luzon arc highlights the importance of relatively enriched components in the lower plate such as terrigenous sediments and seamount basalts that could be introduced into young arc environments (Figure 11c).

5. Concluding Remarks

1. The Oligocene-Pleistocene western Northern Luzon igneous rocks display geochemical characteristics of normal arc magmatism, consistent with derivation from partial melts of mantle wedge coupled with fractional crystallization. In particular, the Oligocene-early Miocene CCDC intrusive rocks exhibit Sr-Nd-Hf-Pb-O isotope composition consistent with mantle metasomatism by fluids/melts released from pelagic sediments. The late Miocene-Pleistocene western Northern Luzon lavas display Sr-Nd-Hf-Pb-O isotope composition, suggestive of mantle metasomatism by fluids/melts released from the subducted Scarborough Seamount Chain basalts.
2. The presence of seamount chain isotopic signatures in western Northern Luzon arc lavas, combined with the dramatic changes in Sr-Nd-Hf-Pb isotopes for the Taiwan-Luzon arc magmatism, marked a transition from the Proto-South China Sea subduction to the South China Sea fossil ridge subduction beneath western Northern Luzon. The enrichment trends in Sr-Nd-Pb isotopes along the Luzon arc also mark the significance of a contribution of relatively enriched components (high Sr-Pb isotopic ratios, low ε_{Nd} values) in the lower plate to the maturation of a juvenile oceanic crust (low Sr-Pb isotopic ratios, high ε_{Nd} values) in a modern arc-continent collision system.

Acknowledgments
This paper was supported by research grants from the National Programme on Global Change and Air-Sea Interaction (GASI-GEOGE-02), National Science Foundation of China (NSFC, 41890812), Key Special Project for Introduced Talents Team of Southern Marine Science and Engineering Guangdong Laboratory (Guangzhou; GML2019ZD0202), Strategic Priority Research Program (B) of Chinese Academy of Sciences (Grant XDB18000000), NSFC (41625007, 41406058, 41973011), State Key Laboratory of Isotope Geochemistry, Guangzhou Institute of Geochemistry, Chinese Academy of Sciences (SKLabIG-KF-16-13), and China Ocean Mineral R&D Association (COMRA) project (DY135-G2-1-01). We would like to thank Pete Hollings and an anonymous reviewer for their detailed, constructive and encouraging reviews, which substantially helped to improve the manuscript, and Professor John Geissman for his editorial handling of this paper. The data used can be found at https://doi.org/10.17632/m6pny2w23t.2 This study represents a compilation of the contributions of many people. Qing Yang, Ya-Nan Yang, Le Zhang, Xin Li, Wei Li, and Meng-Ming Yu are heartily thanked for helping in field and experimental work. Qi Zhao helped draft Figure 1a. This is contribution No. IS-2780 from GIGCAS.

References

Bachman, S. B., Lewis, S. D., & Schweller, W. J. (1983). Evolution of a forearc basin, Luzon central valley, Philippines. *American Association of Petroleum Geologists*, *67*(7), 1143–1162.

Balce, G. R., Encina, R. Y., Momongan, A., & Lara, L. (1980). Geology of the Baguio district and its implications on the tectonic development of the Luzon Central Cordillera. *Geology and Paleontology of Southeast Asia*, *21*, 265–287.

Bellon, H., & Yumul, G. P. (2000). Mio-Pliocene magmatism in the Baguio Mining District (Luzon, Philippines): Age clues to its geodynamic setting. *Comptes Rendus De L Académie Des Sciences Serie Ii Fascicule a-Sciences De La Terre Et Des Planetes*, *331*(4), 295–302. https://doi.org/10.1016/s1251-8050(00)01415-4

Bellon, H., & Yumul, G. P. Jr (2001). Miocene to Quaternary adakites and related rocks in Western Philippine arc sequences. *Comptes Rendus De L Académie des Sciences - Series IIA - Earth and Planetary Science*, *333*(6), 343–350.

Bernard, A., U. Knittel, B. Weber, D. Weis, A. Albrecht, K. Hattori, et al. (1996), Petrology and geochemistry of the 1991 eruption products of Mount Pinatubo, Fire and mud: Eruptions and lahars of Mount Pinatubo, Philippines, 767-797.

Bindeman, I. N., Eiler, J. M., Yogodzinski, G. M., Tatsumi, Y., Stern, C. R., Grove, T. L., et al. (2005). Oxygen isotope evidence for slab melting in modern and ancient subduction zones. *Earth & Planetary Science Letters*, *235*(3), 480–496.

Briais, A., Patriat, P., & Tapponnier, P. (1993). Updated interpretation of magnetic anomalies and seafloor spreading stages in the south China Sea: Implications for the Tertiary tectonics of Southeast Asia. *Journal of Geophysical Research*, *98*(B4), 6299–6328. https://doi.org/10.1029/92JB02280

Castillo, P. R. (1996). Origin and geodynamic implication of the Dupal isotopic anomaly in volcanic rocks from the Philippine island arcs. *Geology*, *24*(3), 271–274. https://doi.org/10.1130/0091-7613(1996)024<0271:oagiot>2.3.co;2

Castillo, P. R. (2012). Adakite petrogenesis. *Lithos*, *134*, 304–316. https://doi.org/10.1016/j.lithos.2011.09.013

Castillo, P. R., Janney, P. E., & Solidum, R. U. (1999). Petrology and geochemistry of Camiguin Island, southern Philippines: Insights to the source of adakites and other lavas in a complex arc setting. *Contributions to Mineralogy and Petrology*, *134*(1), 33–51.

Chen, C.-H., Shieh, Y.-N., Lee, T., Chen, C.-H., & Mertzman, S. A. (1990). Nd-Sr-O isotopic evidence for source contamination and an unusual mantle component under Luzon Arc. *Geochimica et Cosmochimica Acta*, *54*(9), 2473–2483. https://doi.org/10.1016/0016-7037(90)90234-C

Chung, S.-L., Liu, D., Ji, J., Lo, C.-H., Wen, D.-J., Lee, H.-Y., et al. (2003). Adakites from continental collision zones: Melting of thickened lower crust beneath southern Tibet. *Geology*, *31*(11), 1021–1024. https://doi.org/10.1130/g19796.1

Cooke, D. R., & Bloom, M. S. (1990). Epithermal and subjacent porphyry mineralization, Acupan, Baguio District, Philippines: A fluid-inclusion and paragenetic study. *Journal of Geochemical Exploration*, *35*(1), 297–340.

Defant, M. J., & Drummond, M. S. (1990). Derivation of some modern arc magmas by melting of young subducted lithosphere. *Nature*, *347*(6294), 662–665.

Defant, M. J., Jacques, D., Mairu, R. C., De Boer, J., & Joron, J.-L. (1989). Geochemistry and tectonic setting of the Luzon arc, Philippines. *Geological Society of America Bulletin*, *101*(5), 663–672. https://doi.org/10.1130/0016-7606(1989)101<0663:gatsot>2.3.co;2

Delacour, A., Frueh-Green, G. L., Frank, M., Gutjahr, M., & Kelley, D. S. (2008). Sr- and Nd-isotope geochemistry of the Atlantis Massif (30 degrees N, MAR): Implications for fluid fluxes and lithospheric heterogeneity. *Chemical Geology*, *254*(1-2), 19–35. https://doi.org/10.1016/j.chemgeo.2008.05.018

Dimalanta, C. B., & Yumul, J. G. P. (2008). Crustal thickness and adakite occurrence in the Philippines: Is there a relationship? *Island Arc*, *17*(4), 421–431.

Ding, W., & Li, J. (2016). Propagated rifting in the Southwest Sub-basin, South China Sea: Insights from analogue modelling. *Journal of Geodynamics*, *100*, 71–86.

Ding, W., Sun, Z., Dadd, K., Fang, Y., & Li, J. (2018). Structures within the oceanic crust of the central South China Sea basin and their implications for oceanic accretionary processes. *Earth & Planetary Science Letters*, *488*, 115–125.

Ducea, M. N., Saleeby, J. B., & Bergantz, G. (2015). The Architecture, Chemistry, and Evolution of Continental Magmatic Arcs. *Annual Review of Earth and Planetary Sciences*, *43*(1), 299–331. https://doi.org/10.1146/annurev-earth-060614-105049

DuFrane, S. A., Asmerom, Y., Mukasa, S. B., Morris, J. D., & Dreyer, B. M. (2006). Subduction and melting processes inferred from U-Series, Sr-Nd-Pb isotope, and trace element data, Bicol and Bataan arcs, Philippines. *Geochimica et Cosmochimica Acta*, *70*(13), 3401–3420.

Elburg, M. A., Bergen, M. J. V., & Foden, J. D. (2004). Subducted upper and lower continental crust contributes to magmatism in the collision sector of the Sunda-Banda arc, Indonesia. *Geology*, *32*(1), 41–44.

Encarnación, J., Mukasa, S. B., & Evans, C. A. (1999). Subduction components and the generation of arc-like melts in the Zambales ophiolite, Philippines: Pb, Sr and Nd isotopic constraints. *Chemical Geology*, *156*(1–4), 343–357. https://doi.org/10.1016/S0009-2541(98)00190-9

Encarnación, J. P., Mukasa, S. B., & Obille, E. C. (1993). Zircon U-Pb geochronology of the Zambales and Angat Ophiolites, Luzon, Philippines: Evidence for an Eocene arc-back arc pair. *Journal of Geophysical Research*, *98*(B11), 19991–20004.

Fan, J., Zhao, D., Dong, D., & Zhang, G. (2017). P-wave tomography of subduction zones around the central Philippines and its geodynamic implications. *Journal of Asian Earth Sciences*, *146*(Supplement C), 76–89. https://doi.org/10.1016/j.jseaes.2017.05.015

Fan, J. K., Wu, S. G., & Spence, G. (2014). Tomographic evidence for a slab tear induced by fossil ridge subduction at Manila Trench, South China Sea. *International Geology Review*, *57*(5-8), 998–1013.

Gao, X., Zhang, J., Sun, Y. J., & Wu, S. G. (2012). A simulation study on the thermal structure of Manila trench subduction zone. *Chinese Journal of Geophysics*, *55*(1), 117–125 (in Chinese with English abstract). https://doi.org/10.6038/j.issn.0001-5733.2012.01.011

Hall, R. (2012). Late Jurassic–Cenozoic reconstructions of the Indonesian region and the Indian Ocean. *Tectonophysics*, *570-571*, 1–41. https://doi.org/10.1016/j.tecto.2012.04.021

Hall, R., & Breitfeld, T. (2017). Nature and demise of the Proto-South China Sea. *Bulletin of the Geological Society of Malaysia*, *63*, 61–76.

Hart, S. R. (1984). A large-scale isotope anomaly in the Southern-Hemisphere mantle. *Nature*, *309*(5971), 753–757. https://doi.org/10.1038/309753a0

Hayes, D. E., & Lewis, S. D. (1984). A geophysical study of the Manila Trench, Luzon, Philippines: 1. Crustal structure, gravity, and regional tectonic evolution. *Journal of Geophysical Research*, *89*(B11), 9171–9195. https://doi.org/10.1029/JB089iB11p09171

Hickey-Vargas, R., Bizimis, M., & Deschamps, A. (2008). Onset of the Indian Ocean isotopic signature in the Philippine Sea Plate: Hf and Pb isotope evidence from Early Cretaceous terranes. *Earth and Planetary Science Letters*, *268*(3–4), 255–267. https://doi.org/10.1016/j.epsl.2008.01.003

Hinz, K., Block, M., Kudrass, H. R., & Meyer, H. (1991). Structural elements of the Sulu Sea, Phillipines. *Geologisches Jahrbuch*, *127*, 483–506.

Hollings, P., Cooke, D. R., Waters, P. J., & Cousens, B. (2011). Igneous geochemistry of mineralized rocks of the Baguio District, Philippines: Implications for tectonic evolution and the genesis of porphyry-style mineralization. *Economic Geology*, *106*(8), 1317–1333.

Hollings, P., Sweet, G., Baker, M., Cooke, D. R., Friedman, R., Colpron, M., . . . Thompson, J. F. H. (2013). Tectonomagmatic controls on porphyry mineralization: Geochemical evidence from the Black Mountain porphyry system, Philippines *Tectonics, Metallogeny, and Discovery: The North American Cordillera and Similar Accretionary Settings* (Vol. 17, pp. 0): Society of Economic Geologists.

Hollings, P., Wolfe, R., Cooke, D. R., & Waters, P. J. (2011). Geochemistry of Tertiary igneous rocks of Northern Luzon, Philippines: Evidence for a back-arc setting for alkalic porphyry copper-gold deposits and a case for slab roll-back? *Economic Geology*, *106*(8), 1257–1277.

Huang, C.-Y., Wu, W.-Y., Chang, C.-P., Tsao, S., Yuan, P. B., Lin, C.-W., & Xia, K.-Y. (1997). Tectonic evolution of accretionary prism in the arc-continent collision terrane of Taiwan. *Tectonophysics*, *281*(1), 31–51. https://doi.org/10.1016/S0040-1951(97)00157-1

Huang, W., & Wang, P. X. (2006). Sediment mass and distribution in the South China Sea since the Oligocene. *Science China Earth Sciences*, *49*(11), 1147–1155. https://doi.org/10.1007/s11430-006-2019-4

Huchon, P., Nguyen, T. N. H., & Chamot-Rooke, N. (2001). Propagation of continental break-up in the southwestern South China Sea. *Geological Society, London, Special Publications*, *187*(1), 31–50. https://doi.org/10.1144/gsl.sp.2001.187.01.03

Hutchison, C. S. (2010). The North-West Borneo Trough. *Marine Geology*, *271*(1–2), 32–43.

Jahn, B.-M. (2004). The Central Asian Orogenic Belt and growth of the continental crust in the Phanerozoic. *Geological Society, London, Special Publications*, *226*(1), 73–100. https://doi.org/10.1144/gsl.sp.2004.226.01.05

Jégo, S., Maury, R. C., Polvé, M., Yumul, G. P., Bellon, H., Tamayo, R. A., & Cotten, J. (2005). Geochemistry of adakites from the Philippines: Constraints on their origins. *Resource Geology*, *55*(3), 163–188. https://doi.org/10.1111/j.1751-3928.2005.tb00239.x

Kay, R. W. (1978). Aleutian magnesian andesites: Melts from subducted Pacific ocean crust. *Journal of Volcanology and Geothermal Research*, *4*, 117–132.

Kelley, K. A., Plank, T., Grove, T. L., Stolper, E. M., Newman, S., & Hauri, E. (2006). Mantle melting as a function of water content beneath back-arc basins. *Journal of Geophysical Research*, *111*, B09208. https://doi.org/10.1029/2005jb003732

Knittel, U., & Defant, M. J. (1988). Sr isotopic and trace element variations in Oligocene to recent igneous rocks from the Philippine island arc: Evidence for recent enrichment in the sub-Philippine mantle. *Earth and Planetary Science Letters*, *87*(1), 87–99. https://doi.org/10.1016/0012-821X(88)90066-0

Knittel, U., Defant, M. J., & Raczek, I. (1988). Recent enrichment in the source region of arc magmas from Luzon island, Philippines: Sr and Nd isotopic evidence. *Geology*, *16*(1), 73–76. https://doi.org/10.1130/0091-7613(1988)016<0073:reitsr>2.3.co;2

Knittel, U., & Yang, T. F. (1998). Source components and enrichment processes in the mantle wedge beneath Luzon (Philippines). In *Mantle dynamics and plate interactions in East Asia*, (pp. 403–385). Washington, DC: American Geophysical Union. https://doi.org/10.1029/GD027p0385

Lai, Y. M., Song, S. R., Lo, C. H., Lin, T. H., Chu, M. F., & Chung, S. L. (2017). Age, geochemical and isotopic variations in volcanic rocks from the Coastal Range of Taiwan: Implications for magma generation in the Northern Luzon Arc. *Lithos*, *272*, 92–115. https://doi.org/10.1016/j.lithos.2016.11.012

Li, C.-F., Xu, X., Lin, J., Sun, Z., Zhu, J., Yao, Y., et al. (2014). Ages and magnetic structures of the South China Sea constrained by deep tow magnetic surveys and IODP Expedition 349. *Geochemistry, Geophysics, Geosystems*, *15*, 4958–4983. https://doi.org/10.1002/2014GC005567

Li, J., Jin, X., Aiguo, R., Wu, S., Wu, Z., & Liu, J. (2004). Indentation tectonics in the accretionary wedge of middle Manila Trench. *Chinese Science Bulletin*, *49*(12), 1279–1288.

Li, X.-H., Li, W.-X., Li, Q.-L., Wang, X.-C., Liu, Y., & Yang, Y.-H. (2010). Petrogenesis and tectonic significance of the ~850 Ma Gangbian alkaline complex in South China: Evidence from in situ zircon U–Pb dating, Hf–O isotopes and whole-rock geochemistry. *Lithos*, *114*(1), 1–15. https://doi.org/10.1016/j.lithos.2009.07.011

Li, X. H., Liu, Y., Li, Q. L., Guo, C. H., & Chamberlain, K. R. (2009). Precise determination of Phanerozoic zircon Pb/Pb age by multicollector SIMS without external standardization. *eochemistry, Geophysics, Geosystems*, *10*, Q04010. https://doi.org/10.1029/2009GC002400

Li, X. H., Long, W. G., Li, Q. L., Liu, Y., Zheng, Y. F., Yang, Y. H., et al. (2010). Penglai zircon megacrysts: A potential new working reference material for microbeam determination of Hf–O Isotopes and U–Pb age. *Geostandards & Geoanalytical Research*, *34*(2), 117–134. https://doi.org/10.1111/j.1751-908X.2010.00036.x

Li, X. H., Tang, G. Q., Gong, B., Yang, Y. H., Hou, K. J., Hu, Z. C., et al. (2013). Qinghu zircon: A working reference for microbeam analysis of U-Pb age and Hf and O isotopes. *Chinese Science Bulletin*, *58*(36), 4647–4654.

Li, X. H., Wei, G., Shao, L., Liu, Y., Liang, X., Jian, Z., et al. (2003). Geochemical and Nd isotopic variations in sediments of the South China Sea: A response to Cenozoic tectonism in SE Asia ☆. *Earth & Planetary Science Letters*, *211*(3–4), 207–220.

Ludwig, K. R. (2003). ISOPLOT 3: A geochronological Toolkit for Microsoft excel. *Berkeley Geochronology Centre Special Publication*, *4*, 74.

Macpherson, C. G., Dreher, S. T., & Thirlwall, M. F. (2006). Adakites without slab melting: High pressure differentiation of island arc magma, Mindanao, the Philippines. *Earth and Planetary Science Letters*, *243*(3-4), 581–593.

Marini, J.-C., Chauvel, C., & Maury, R. C. (2005). Hf isotope compositions of northern Luzon arc lavas suggest involvement of pelagic sediments in their source. *Contributions to Mineralogy and Petrology*, *149*(2), 216–232. https://doi.org/10.1007/s00410-004-0645-4

McDermott, F., Defant, M. J., Hawkesworth, C. J., Maury, R. C., & Joron, J. L. (1993). Isotope and trace element evidence for three component mixing in the genesis of the North Luzon arc lavas (Philippines). *Contributions to Mineralogy and Petrology*, *113*(1), 9–23.

Mckenzie, D., & O'Nions, R. K. (1991). Partial melt distributions from inversion of rare Earth element concentrations. *Journal of Petrology*, *32*(6), 1021–1091.

Middlemost, E. A. K. (1994). Naming materials in the magma/igneous rock system. *Earth-Science Reviews*, *37*(3), 215–224. https://doi.org/10.1016/0012-8252(94)90029-9

Miyazaki, T., & Shuto, K. (1998). Sr and Nd isotope ratios of twelve GSJ rock reference samples. *Geochemical Journal*, *32*(5), 345–350.

Mukasa, S. B., Flower, M. F. J., & Miklius, A. (1994). The Nd-, Sr- and Pb-isotopic character of lavas from Taal, Laguna de Bay and Arayat volcanoes, southwestern Luzon, Philippines: Implications for arc magma petrogenesis. *Tectonophysics*, *235*(1–2), 205–221. https://doi.org/10.1016/0040-1951(94)90024-8

Mukasa, S. B., McCabe, R., & Gill, J. B. (1987). Pb-isotopic compositions of volcanic rocks in the West and East Philippine island arcs: Presence of the Dupal isotopic anomaly. *Earth and Planetary Science Letters*, *84*(2–3), 153–164. https://doi.org/10.1016/0012-821X(87)90082-3

Pautot, G., & Rangin, C. (1989). Subduction of the South China Sea axial ridge below Luzon (Philippines). *Earth & Planetary Science Letters*, *92*(1), 57–69.

Payot, B. D., Jego, S., Maury, R. C., Polve, M., Gregoire, M., Ceuleneer, G., et al. (2007). The oceanic substratum of Northern Luzon: Evidence from xenoliths within Monglo adakite (the Philippines). *Island Arc*, *16*(2), 276–290. https://doi.org/10.1111/j.1440-1738.2007.00574.x

Peña, R. E. (1998). Further notes on the stratigraphy of the Baguio district. *Journal of the Geological Society of the Philippines*, *53*, 141–157.

Plank, T., & Langmuir, C. H. (1998). The chemical composition of subducting sediment and its consequences for the crust and mantle. *Chemical Geology*, *145*(3-4), 325–394.

Polve, M., Maury, R. C., Jego, S., Bellon, H., Margoum, A., Yumul, G. P., et al. (2007). Temporal geochemical evolution of Neogene magmatism in the Baguio Gold–Copper Mining District (Northern Luzon, Philippines). *Resource Geology*, *57*(2), 197–218. https://doi.org/10.1111/j.1751-3928.2007.00017.x

Qi, L., Hu, J., & Conrad, G. D. (2000). Determination of trace elements in granites by inductively coupled plasma mass spectrometry. *Talanta*, *51*(3), 507–513. https://doi.org/10.1016/S0039-9140(99)00318-5

Queaño, K. L., Ali, J. R., Milsom, J., Aitchison, J. C., & Pubellier, M. (2007). North Luzon and the Philippine Sea Plate motion model: Insights following paleomagnetic, structural, and age-dating investigations. *Journal of Geophysical Research*, *112*, B05101. https://doi.org/10.1029/2006JB004506

Rangin, C., Le Pichon, X., Mazzotti, S., Pubellier, M., Chamot-Rooke, N., Aurelio, M., et al. (1999). Plate convergence measured by GPS across the Sundaland/Philippine Sea Plate deformed boundary: The Philippines and eastern Indonesia. *Geophysical Journal International*, *139*(2), 296–316. https://doi.org/10.1046/j.1365-246x.1999.00969.x

Rapp, R. P., Shimizu, N., Norman, M. D., & Applegate, G. S. (1999). Reaction between slab-derived melts and peridotite in the mantle wedge: Experimental constraints at 3.8 GPa. *Chemical Geology*, *160*(4), 335–356. https://doi.org/10.1016/S0009-2541(99)00106-0

Rapp, R. P., & Watson, E. B. (1995). Dehydration melting of metabasalt at 8–32 kbar: Implications for continental growth and crust-mantle recycling. *Journal of Petrology*, *36*(4), 891–931. https://doi.org/10.1093/petrology/36.4.891

Rapp, R. P., Watson, E. B., & Miller, C. F. (1991). Partial melting of amphibolite/eclogite and the origin of Archean trondhjemites and tonalites. *Precambrian Research*, *51*(1), 1–25. https://doi.org/10.1016/0301-9268(91)90092-O

Rollison, H. R. (1993). *Using Geochemical Data: Evaluation, Presentation, Interpretation* (352 pp.). Singapore: Longman.

Schafer, P. (1954). Some phases of the geology of the Baguio district. *Mining Newsletter*, Manilla, *5*, 5–7.

Sen, C., & Dunn, T. (1994). Dehydration melting of a basaltic composition amphibolite at 1.5 and 2.0 GPa: Implications for the origin of adakites. *Contributions to Mineralogy and Petrology*, *117*(4), 394–409. https://doi.org/10.1007/bf00307273

Sengör, A. M. C., Natal'in, B. A., & Burtman, V. S. (1993). Evolution of the Altaid tectonic collage and Palaeozoic crustal growth in Eurasia. *Nature*, *364*(6435), 299–307.

Shannon, J. R. (1979), Igneous petrology, geochemistry and fission track ages of a portion of the Baguio district, Northern Luzon, Philippines, *Unpublished M. Sc. thesis, Golden, Colorado, Colorado School of Mines*, 173.

Shao, W.-Y., Chung, S.-L., Chen, W.-S., Lee, H.-Y., & Xie, L.-W. (2015). Old continental zircons from a young oceanic arc, eastern Taiwan: Implications for Luzon subduction initiation and Asian accretionary orogeny. *Geology*, *43*(6), 479–482. https://doi.org/10.1130/g36499.1

Shimoda, G., Tatsumi, Y., Nohda, S., Ishizaka, K., & Jahn, B. M. (1998). Setouchi high-Mg andesites revisited: Geochemical evidence for melting of subducting sediments. *Earth and Planetary Science Letters*, *160*(3–4), 479–492. https://doi.org/10.1016/S0012-821X(98)00105-8

Sigmarsson, O., Chmeleff, J., Morris, J., & Lopez-Escobar, L. (2002). Origin of 226Ra–230Th disequilibria in arc lavas from southern Chile and implications for magma transfer time. *Earth and Planetary Science Letters*, *196*(3), 189–196. https://doi.org/10.1016/S0012-821X(01)00611-2

Sigmarsson, O., Martin, H., & Knowles, J. (1998). Melting of a subducting oceanic crust from U-Th disequilibria in austral Andean lavas. *Nature*, *394*(6693), 566–569.

Sláma, J., Košler, J., Condon, D. J., Crowley, J. L., Gerdes, A., Hanchar, J. M., et al. (2008). Plesovice zircon—A new natural reference material for U-Pb and Hf isotopic microanalysis. *Chemical Geology*, *249*(1-2), 1–35. https://doi.org/10.1016/j.chemgeo.2007.11.005

Solidum, R. U., Castillo, P. R., & Hawkins, J. W. (2003). Geochemistry of lavas from Negros Arc, west central Philippines: Insights into the contribution from the subducting slab. *Geochemistry, Geophysics, Geosystems*, *4*(10), 9008. https://doi.org/10.1029/2003GC000513

Stern, C. R., & Kilian, R. (1996). Role of the subducted slab, mantle wedge and continental crust in the generation of adakites from the Andean Austral Volcanic Zone. *Contributions to Mineralogy and Petrology*, *123*(3), 263–281. https://doi.org/10.1007/s004100050155

Sun, S.-S. (1980). Lead isotopic study of young volcanic rocks from mid-ocean ridges, ocean islands and island arcs. *Philosophical Transactions of the Royal Society of London. Series A, Mathematical and Physical Sciences*, *297*(1431), 409–445. https://doi.org/10.1098/rsta.1980.0224

Sun, S. S., & McDonough, W. F. (1989). Chemical and isotopic systematics of oceanic basalts: Implications for mantle composition and processes. *Geological Society, London, Special Publications*, *42*(1), 313–345. https://doi.org/10.1144/gsl.sp.1989.042.01.19

Tanaka, T., Togashi, S., Kamioka, H., Amakawa, H., Kagami, H., Hamamoto, T., et al. (2000). JNdi-1: A neodymium isotopic reference in consistency with LaJolla neodymium. *Chemical Geology*, *168*(3), 279–281. https://doi.org/10.1016/S0009-2541(00)00198-4

Tang, G.-J., Wang, Q., Wyman, D. A., & Dan, W. (2019). Crustal maturation through chemical weathering and crustal recycling revealed by Hf–O–B isotopes. *Earth and Planetary Science Letters*, *524*. https://doi.org/10.1016/j.epsl.2019.115709

Tang, Q., & Zheng, C. (2013). Crust and upper mantle structure and its tectonic implications in the South China Sea and adjacent regions. *Journal of Asian Earth Sciences*, *62*, 510–525.

Taylor, B., & Hayes, D. E. (1980). The tectonic evolution of the South China basin. *Tectonic & Geologic Evolution of Southeast Asian Seas & Islands*, *23*, 89–104.

Taylor, B., & Hayes, D. E. (1983). *Origin and history of the South China Sea basin, in The tectonic and geologic evolution of Southeast Asian seas and islands: Part 2*, (pp. 23–56). Washington, DC: American Geophysical Union.

Taylor, S. R., McLennan, S. M., & McCulloch, M. T. (1983). Geochemistry of loess, continental crustal composition and crustal model ages. *Geochimica et Cosmochimica Acta*, *47*(11), 1897–1905. https://doi.org/10.1016/0016-7037(83)90206-5

Teng, L. S. (1990). Geotectonic evolution of late Cenozoic arc-continent collision in Taiwan. *Tectonophysics*, *183*(1), 57–76.

Tsai, Y. B., Liaw, Z. S., Lee, T. Q., Lin, M. T., & Yeh, Y. H. (1981). Seismological evidence of an active plate boundary in the Taiwan area. *Memoir of the Geological Society of China*, *4*(143-154).

Tu, K., Flower, M. F. J., Carlson, R. W., Xie, G., Chen, C.-Y., & Zhang, M. (1992). Magmatism in the South China Basin: 1. Isotopic and trace-element evidence for an endogenous Dupal mantle component. *Chemical Geology*, *97*(1–2), 47–63. https://doi.org/10.1016/0009-2541(92)90135-R

Valley, J. W., Lackey, J. S., Cavosie, A. J., Clechenko, C. C., Spicuzza, M. J., Basei, M. A. S., et al. (2005). 4.4 billion years of crustal maturation: Oxygen isotope ratios of magmatic zircon. *Contributions to Mineralogy and Petrology*, *150*(6), 561–580. https://doi.org/10.1007/s00410-005-0025-8

Vervoort, J. D., Plank, T., & Prytulak, J. (2011). The Hf–Nd isotopic composition of marine sediments. *Geochimica Et Cosmochimica Acta*, *75*(20), 5903–5926.

Vidal, P., Dupuy, C., Maury, R., & Richard, M. (1989). Mantle metasomatism above subduction zones: Trace-element and radiogenic isotope characteristics of peridotite xenoliths from Batan Island (Philippines). *Geology*, *17*(12), 1115–1118. https://doi.org/10.1130/0091-7613(1989)017<1115:mmaszt>2.3.co;2

Vroon, P. Z., van Bergen, M. J., White, W. M., & Varekamp, J. C. (1993). Sr-Nd-Pb isotope systematics of the Banda Arc, Indonesia: Combined subduction and assimilation of continental material. *Journal of Geophysical Research*, *98*(B12), 22349–22366. https://doi.org/10.1029/93jb01716

Wang, P. (2012). Tracing the life history of a marginal sea—On "The South China Sea Deep" Research Program. *Chinese Science Bulletin*, *57*(24), 3093–3114. https://doi.org/10.1007/s11434-012-5087-1

Wang, P. C., Li, S. Z., Guo, L. L., Jiang, S. H., Somerville, I. D., Zhao, S. J., et al. (2016). Mesozoic and Cenozoic accretionary orogenic processes in Borneo and their mechanisms. *Geological Journal*, *51*(S1), 464–489.

Wang, Q., Wyman, D. A., Xu, J., Jian, P., Zhao, Z., Li, C., et al. (2007). Early Cretaceous adakitic granites in the Northern Dabie Complex, central China: Implications for partial melting and delamination of thickened lower crust. *Geochimica et Cosmochimica Acta*, *71*(10), 2609–2636. https://doi.org/10.1016/j.gca.2007.03.008

Wang, Y. J., Han, X. Q., & Luo, Z. H. (2009). Late Miocene magmatism and evolution of Zhenbei-Huangyan Seamount in the South China Sea: Evidence from petrochemistry and chronology. *Acta Oceanologica Sinica*, *31*(4), 93–102. (in Chinese with English abstract)

Waters, P. J., Cooke, D. R., Gonzales, R. I., & Phillips, D. (2011). Porphyry and epithermal deposits and Ar-40/Ar-39 geochronology of the Baguio District, Philippines. *Economic Geology*, *106*(8), 1335–1363.

Weis, D., Kieffer, B., Maerschalk, C., Pretorius, W., & Barling, J. (2005). High-precision Pb-Sr-Nd-Hf isotopic characterization of USGS BHVO-1 and BHVO-2 reference materials. *Geochemistry, Geophysics, Geosystems*, *6*, Q02002. https://doi.org/10.1029/2004gc000852

Whitehouse, M. J., Claesson, S., Sunde, T., & Vestin, J. (1997). Ion microprobe U-Pb zircon geochronology and correlation of Archaean gneisses from the Lewisian Complex of Gruinard Bay, northwestern Scotland. *Geochimica et Cosmochimica Acta*, *61*(20), 4429–4438.

Winther, K. T., & Newton, R. C. (1991). Experimental melting of hydrous low-K tholeiite: Evidence on the origin of Archean cratons. *Bulletin of the Geological Society of Denmark*, *39*(5), 2932–2945.

Wolfe, J. A. (1988). Arc magmatism and mineralization in North Luzon and its relationship to subduction at the East Luzon and North Manila Trenches. *Journal of Southeast Asian Earth Sciences*, *2*(2), 79–93.

Wu, F.-Y., Yang, Y.-H., Xie, L.-W., Yang, J.-H., & Xu, P. (2006). Hf isotopic compositions of the standard zircons and baddeleyites used in U–Pb geochronology. *Chemical Geology*, *234*(1), 105–126. https://doi.org/10.1016/j.chemgeo.2006.05.003

Wu, J., Suppe, J., Lu, R., & Kanda, R. (2016). Philippine Sea and East Asian plate tectonics since 52 Ma constrained by new subducted slab reconstruction methods. *Journal of Geophysical Research: Solid Earth*, *121*, 4670–4741. https://doi.org/10.1002/2016JB012923

Xu, Y.-G., Wei, J.-X., Qiu, H.-N., Zhang, H.-H., & Huang, X.-L. (2012). Opening and evolution of the South China Sea constrained by studies on volcanic rocks: Preliminary results and a research design. *Chinese Science Bulletin*, *57*(24), 3150–3164.

Yang, T. F., Lee, T., Chen, C.-H., Cheng, S.-N., Knittel, U., Punongbayan, R. S., & Rasdas, A. R. (1996). A double island arc between Taiwan and Luzon: Consequence of ridge subduction. *Tectonophysics*, *258*(1-4), 85–101.

Yuan, Y., Yang, S., Tang, X., Wang, B., Hou, H., & Liu, Z. (1994). Surrounding block kinematics and tectonic evolution of South China Sea since late Mesozoic. *Tropic Oceanology*, *13*(2), 9–16. (in Chinese with English abstract)

Yumul, G. P., Dimalanta, C., Bellon, H., Faustino, D. V., De Jesus, J. V., Tamayo, R. A., & Jumawan, F. T. (2000). Adakitic lavas in the Central Luzon back-arc region, Philippines: Lower crust partial melting products? *Island Arc*, *9*(4), 499–512.

Yumul, G. P., Dimalanta, C. B., Tamayo, R. A., & Bellon, H. (2003). Silicic arc volcanism in Central Luzon, the Philippines: Characterization of its space, time and geochemical relationship. *Island Arc*, *12*(2), 207–218.

Zhang, G.-L., Chen, L.-H., Jackson, M. G., & Hofmann, A. W. (2017). Evolution of carbonated melt to alkali basalt in the South China Sea. *Nature Geoscience*, *10*(3), 229–235. https://doi.org/10.1038/ngeo2877

Zhang, G.-L., Luo, Q., Zhao, J., Jackson, M. G., Guo, L.-S., & Zhong, L.-F. (2018). Geochemical nature of sub-ridge mantle and opening dynamics of the South China Sea. *Earth and Planetary Science Letters*, *489*, 145–155. https://doi.org/10.1016/j.epsl.2018.02.040